

Puckering Free Energy of Pyranoses Using a Combined Metadynamics–Umbrella Sampling Approach

E. Autieri, M. Sega,* and F. Pederiva

*Department of Physics and I.N.F.N., University of Trento,
via Sommarive 14, 38112 Trento, Italy*

Abstract

We present the results of a combined metadynamics–umbrella sampling investigation of the puckered conformers of pyranoses described using the GROMOS 45a4 force field. The free energy landscape of Cremer–Pople puckering coordinates has been calculated for the whole series of α and β aldohexoses. We show that the 45a4 force field parameters fail in reproducing proper free energy differences between chair conformers for many of the inspected monosaccharides. In the extreme cases of galactose, mannose and allose, the experimentally non-detectable inverted chair conformers become even substantially populated. The opposite behavior is observed in the case of idose, which is the only experimentally known aldohexose that shows equilibrium between chair and inverted chair. We suggest a modification to the GROMOS 45a4 parameter set, which improves considerably the accordance of simulation results with theoretical and experimental estimates of puckering free energies.

I. INTRODUCTION

Within the framework of classical force fields, the number of computer experiments on saccharides has grown considerably in recent years, and various systems have been addressed^{1–27}. Devising a realistic model of monosaccharides is obviously a decisive step in order for carbohydrates simulations to have enough predictive power. The accurate description of monosaccharides with classical force fields is not an easy task, because of the delicate interplay of different factors such as the presence of a high number of intramolecular hydrogen bonds, the competition of these hydrogen bonds with water-sugar ones and important steric and electrostatic effects between ring substituents in spatial proximity (see for example Ref. 28 and references within). The problem of reproducing some carbohydrates peculiarities, such as the rotameric distribution of the hydroxymethyl group or the anomeric and exo-anomeric effects, have been addressed in various force fields, and the reader can find some comparative analyses in Refs. 29–31. However, considerably less attention has been devoted so far to the correct reproduction of the ring conformational properties.

Cyclic monosaccharides can appear indeed as puckered rings, and their conformational transitions dramatically alter the equilibrium properties of both single sugar rings as well as those in oligo and polysaccharides³². Despite the large number of possible puckered conformers, many biologically relevant monosaccharides in the pyranoid form appear almost always in one stable puckered conformation, the second most populated state being so unlikely not to be detectable by actual experimental techniques. In spite of that, several authors reported an inappropriate percentage of secondary puckered conformations^{32–37} when modeling carbohydrates using classical force fields such as GROMOS^{34,35,38–41} or OPLS-AA⁴² for simulations in solution. Regarding the latest GROMOS parameter set for carbohydrates (45a4)³⁵ (which incidentally was also tuned to improve the description of puckered conformers with respect to older versions), non-chair conformers have been shown to be accessible during equilibrium simulation runs of β -D-glucose, with a statistical frequency of 0.7%²⁸. A more quantitative analysis has been performed recently, by computing the free energy difference between ring conformers of β -D-glucose⁴³. The prediction of the inverted chair free energy, $\simeq 16.5$ kJ/mol, is almost 10 kJ/mol lower than most theoretical and ab-initio simulation results.

A reparametrization of those force fields which present unphysical ring conformers at equilibrium would be therefore highly desirable. A quantitatively accurate description of

puckering free energies is a key requirement to perform proper simulations of those sugars which show an equilibrium between the two chair forms, but also for out-of-equilibrium simulations of any sugar. Simulated pulling of polysaccharides, for example, has been proven to be an important tool for the interpretation of single molecule force-spectroscopy data^{21,44,45}, although the ring conformational transitions simulated using three different force fields (AMBER94⁴⁶, AMBER-GLYCAM⁴⁷ and CHARMM-ParM22/SU01⁴⁸) led to different interpretation of the same experimental data²¹. Obviously, having control on the reliability of force fields in reproducing puckering properties would certainly improve all these kind of approaches.

Even though the importance of reproducing correctly the population of ring conformers is quite broadly recognized, few attempts were made so far to investigate the problem in a systematic way and to understand the origin of the discrepancy between simulation results and experimental and theoretical findings (see for example Refs. 34,35,49). For this reason, we decided to study, employing a combined metadynamics – umbrella sampling approach⁵⁰, the puckering properties of simple α and β -D-aldopyranoses. We modeled the saccharides using the 45a4 carbohydrate parameter set³⁵ of the GROMOS force field, which shows incorrect population of conformers for many sugars, and we identified a new set of parameters that satisfactorily reproduces the free energies of the main ring conformers.

This paper is organized as follows: in Sec. II the problems related to the determination of puckering free energy landscape will be presented; in Sec. III the combined metadynamics–umbrella sampling will be discussed, as well as the use of Cremer–Pople puckering coordinates^{51,52}, their peculiarities as collective variables, and the simulation details; in Sec. IV the puckering free energy profile obtained with the GROMOS 45a4 force field for β -D-glucose is discussed in detail and compared to recent similar calculations⁴³. In Sec V we present the puckering free energy profiles of the whole α and β series of D-aldohexoses modeled with the GROMOS 45a4 force field, showing that the puckering free energies are so poorly reproduced, that the inverted chair conformers of galactose, mannose and α -D-Glc become significantly populated. Subsequently, we propose a change to the 45a4 parameter set, showing how the free energies obtained with the use of the new parameter set compare favorably with available theoretical and experimental data. Eventually, some concluding remarks are presented in Sec. VI.

II. THE PROBLEM OF PYRANOSSES PUCKERING FREE ENERGY

In this work we are focusing on a particular class of carbohydrates, namely, aldohexoses, saccharides of composition $C_6H_{12}O_6$. Aldohexoses can appear in nature in the form of six-membered, cyclic rings, conventionally known as the pyranose form. Pyranoses are characterized by the presence of five chiral centers located at the five ring carbon atoms. Following the convention of Fig. 1, these chiral carbons are here denoted as C1 (the anomeric carbon atom), C2, C3, C4 and C5 (the configurational carbon atom). This leads to quite a high number ($2^5 = 32$) of diastereoisomers, characterized by the axial or equatorial orientation of ring substituents. Based on the chirality at C1 and C5 it is possible to classify pyranoses into α - and β -pyranoses or L- and D-pyranoses, respectively⁵³. For example, α -D-Glc and β -L-Glc differ from β -D-Glc only by the chirality at C1 and C5, respectively.

For each of these two chiralities, $2^3 = 8$ stereoisomers remain, which are conventionally named⁵³ glucose (Glc), galactose (Gal), mannose (Man), allose (All), altrose (Alt), talose (Tal), gulose (Gul) and idose (Ido). The position of substituents at the chiral centres are reported for convenience in Tab. I, for β -D-aldopyranoses.

Each of these stereoisomers, in turn, can adopt different ring conformations. According to IUPAC recommendations⁵⁴, the conformation with two parallel ring sides (four coplanar atoms) and the other two atoms at opposite side of the ring plane is called *chair*. Chair conformers occur in two forms: the one with C4 and C1 respectively above and below the plane defined by the other four atoms, is identified by the symbol 4C_1 , while the conformer showing C1 above the ring plane and C4 below it is denoted by the symbol 1C_4 and often called *inverted chair*. Other puckered conformers with four coplanar atoms exist, such as the so-called *boat* and *skew-boat* (the latter also known as twist-boat). In the case of boats, two parallel ring sides define the ring plane and the atoms at the extrema of the ring are either above or below the ring plane (indicated for examples as 3,0B or $B_{3,0}$); in the case of skew-boats the ring plane is defined by three adjacent atoms and the nonadjacent one with the other ring atoms at opposite side (e.g. 3S_1) of the ring plane. Some ring conformations are depicted in Fig. 2.

Conformers other than the one listed so far, which are of some relevance, are also given a conventional name, such as in the case of envelopes or of half chairs, and the reader can find an exhaustive list in Ref. 54. Obviously, many of the possible conformations are not likely to

contribute significantly to the chemistry and physics of monosaccharides. For pyranoses, only the 4C_1 and 1C_4 conformations happen to be eligible to be the most stable conformations, that is, global minima which are well separated in energy from neighbouring local ones. Other conformers such as boats and skew-boats can in principle appear as local, scarcely populated minima, while half-chairs and envelopes usually correspond to maxima or saddle points and are typical transition states between boats and chairs.

The concept of puckering in rings (specifically, in six-membered rings) dates back to the studies of Sachse^{55,56} on cyclohexane in the late nineteenth century, and has been later applied also to saccharidic rings⁵⁷. Although it was clear that the most stable conformers could have been only either of the two chairs, lack of quantitative information on their relative abundance stimulated many theoretical approaches (for an historical review the reader can look at Ref. 58). Semiempirical approaches accounting for the Hassel-Ottar effect (instability of 1,3-diaxial hydroxymethyl – hydroxyl conformation) and other instability factors introduced by Reeves and Kelly⁵⁹⁻⁶¹ allowed to understand that for most pyranoses the 1C_4 conformation, rather than the 4C_1 , is the most stable one, while in few cases an equilibrium between the two is possible. A quantitative estimate of the free energy difference between puckered conformers in aqueous solution (and not, as it is sometimes erroneously reported, in vacuum) came first with the analysis performed by Angyal who assigned, employing again an empirical scheme, specific free energy contributions to the different destabilizing interactions. The various terms were derived from measured equilibria in solution of cyclitols with their borate complexes⁶². Later, employing a molecular-mechanical approach, Vijayalakshmi and Rao⁶³ obtained other estimates, which were anyway compatible with the inverted chair free energies predicted by Angyal.

Semiempirical methods have been in general a quite successful approach for determining the stereochemical properties of numerous cyclic compounds⁶⁴. Unfortunately, experimental estimates of the ring conformational free energy are not feasible for many pyranoses, mostly because the populations of the less stable conformers are usually too tiny to be detected with probes such as NMR^{65,66}. For some pyranoses, however, the destabilizing effects in the 4C_1 and 1C_4 conformations are similar and, as in the case of idose, the relative population of these two conformers becomes an experimentally accessible quantity. Indeed, in Refs. 62,63 the free energy differences estimated for α -D-Ido and β -D-Ido were proven to be compatible with the experimental findings obtained by Snyder and Serianni years later⁶⁷ (see Tab. II).

The accordance with experiment is within $\simeq 4\text{kJ/mol}$, but these results are of particular significance because they correctly predicted the preference of $\alpha\text{-D-Ido}$ for the inverted chair conformer.

The only other pyranose for which experimental measurement of inverted chair population via NMR could be feasible is altrose. Some NMR conformational studies regarding $\alpha\text{-D-Alt}$ in macrocycles^{68,69} in solution show indeed that ${}^4\text{C}_1, {}^1\text{C}_4$, and ${}^{\text{O}}\text{S}_2$ have roughly the same population. To the best of our knowledge, however, no results about altrose monosaccharide conformer populations have ever been published (NMR measurements on altrose are currently being carried on in our laboratory, and preliminary results⁷⁰ seems to be compatible with the theoretical predictions of Refs. 62 and 63). For the other pyranoses considered in this work, only lower bounds can in principle be determined from the sensitivity of experimental probes. In this sense, semi-empirical methods predict correctly the extremely high free energy of inverted chairs of glucose, galactose and mannose.

Some more recent experiments involving atomic force microscope (AFM) spectroscopy have allowed researchers to estimate the puckering free energy of conformers different from the chair ones. Marszalek, Lee, and coworkers^{44,71,72}, for example, estimated the puckering free energy of glucose twisted boats employing AFM pulling on dextran, an $\alpha\text{-(1}\rightarrow\text{6)}$ linked glucan. The conformational changes involved in the elongation of this polysaccharide are quite complex, involving ring deformation due to its intrinsic elasticity, rotations around the C5–C6 bond and chair to twisted boat transitions. In order to isolate these different contributions, the authors performed AFM pulling also on $\beta\text{-(1}\rightarrow\text{4)}$ -D-Glc (cellulose) and on a $\beta\text{-(1}\rightarrow\text{6)}$ linked glucan, namely, pustulan. These polysaccharides are both homopolymers of glucose like dextran but in the elongation process, due to the particular linkages, cellulose presents (apart from chain flexibility) only ring deformation, while pustulan presents both ring deformation and rotation around the C5–C6 bond, but no transition to the twisted boat conformer. By subtracting the free energy differences related to the various processes, the puckering free energy of the glucose twist boat was estimated to be about 25 kJ/mol ⁷². It is worth mentioning, that AFM spectroscopy was first employed to estimate puckering free energies of glucose boats conformers on carboxymethyl amylose (CMA) by Marszalek and coworkers⁷³, and Li and coworkers⁷⁴, independently. The two groups reported values of the boat free energy which were in agreement and in the range $15 - 18\text{ kJ/mol}$. These results differ considerably from the estimate of twisted boat free energy obtained from the analysis

of force-extension curves of dextran. However, CMA — oppositely to dextran, which has no intrinsic torsion — adopts preferentially a pseudo-helical conformation, and this has already been pointed out in Ref. 71 to be a possible source of error when using freely jointed chain models to interpret data. More recently, Kuttel and Naidoo⁷⁵ suggested that in amylose stretching the elongation might be due to a complex rotation of glycosidic linkages, and that chair to boat transitions could play little role in the process. Finally we would like to mention that 4C_1 to 1C_4 transitions could be in principle investigated by means of AFM spectroscopy of, *e.g.*, pectin⁷¹. Their more complex two-step transition prevented so far an estimate of the puckering free energy, but it still represents — to the best of our knowledge — the only approach which could provide direct estimate of inverted chair free energies of the pyranoid form of aldohexoses other than idose and altrose.

In the field of computer simulations, ab-initio predictions of the puckering free energy of pyranoses are even more scarce: we are only aware of a Car-Parrinello metadynamics of glucose in vacuum⁷⁶ (where, unfortunately, use of non-optimal collective variables has been made of⁷⁷), a Hartree-Fock/coupled clusters calculation (MP2/cc-pVTZ) with inclusion of vibrational, rotational and solvation free energies contributions⁷⁸, and a calculation at the B3LYP/6-311++G** level⁷⁹. The calculations of Appell and coworkers⁷⁹ predicted a free energy difference for the 1C_4 conformer of α -D-Glc and β -D-Glc of 20.40 and 29.18 kJ/mol, respectively. It has to be noticed, that calculations performed by including solvation effects, although only at the MP2/cc-pVTZ level⁷⁸ led to a free energy of β -D-Glc 1C_4 conformer of about 57 kJ/mol. This very estimate appears to be substantially higher than all other ones reported so far. In absence of similar ab-initio calculations for idose, that could be employed as benchmark system, it is in our opinion difficult to assess the confidence level of this estimate. However, the possibility that the values reported in Ref. 62 and Ref. 63 could underestimate the free energy of inverted chairs for stereoisomers other than idose can not be completely ruled out.

Given the results briefly reviewed so far, it is obvious that clear-cut experimental reference values for sugar ring puckering free energies are not yet available. The theoretical estimates presented in Ref. 62 and in Ref. 63 are mutually consistent, in agreement with recent ab-initio calculations⁷⁹, and were able to predict with reasonable accuracy the population of chairs in α , β -D-Ido, and possibly altrose⁷⁰. The results of AFM pulling on dextran are also compatible with these estimates, in the sense that the free energy of boat conformers is expected to be

not lower than that of inverted chairs. On the other hand, some results appear to be not compatible with this set of estimates. An ab-initio calculation⁷⁸ assigned a much higher free energy to glucose inverted chairs, while other data from AFM spectroscopy of CMA^{73,74} go into the opposite direction. By and large, we feel confident that the two series^{62,63} represent reasonable approximations of pyranoses free energy difference between chair conformers, and in this work we will use these values as a reference when testing new force field parameter sets.

III. METHODS

A. Refining Metadynamics with Umbrella Sampling

The term metadynamics identifies a number of techniques that have been devised during the last decade to accelerate dynamics for systems displaying meta-stabilities. Various, slightly different algorithms have been proposed in literature, that exploit the same underlying idea of the first metadynamics implementation⁸⁰ (sometimes referred to as *discrete* metadynamics): the Lagrangian version⁸¹, which relied on the introduction of fictitious degrees of freedom associated to the reaction coordinates; the *direct* metadynamics⁸², which is probably the most employed variant; the well-tempered metadynamics⁸³, which assures a convergent estimate of the free energy profile. All these variants share the usage of a time-dependent biasing potential, $U_{\text{bias}}[s(x), t]$, to ease the exploration of the phase space along suitably chosen collective variables, $s(x)$, in turn themselves functions of the atomic coordinates x . The collective variables must represent all slow degrees of freedom characterizing the system, in order for metadynamics – as well as any other free energy profile reconstruction method – to be meaningful⁸⁴.

The direct metadynamics approach shares many traits with other enhanced sampling methods, such as the Local Elevation method⁸⁵ or the adaptive umbrella sampling⁸⁶ (detailed lists of enhanced sampling techniques based on molecular dynamics can be found in Refs. 43 and 84), but the fact that the free energy landscape in metadynamics is usually estimated as the negative of the biasing potential in a single, out-of-equilibrium sweep, makes the technique susceptible, at least in principle, of errors introduced by the deposition protocol. Distinct approaches have been devised to estimate the statistical and systematic errors in

metadynamics, and also to recover a truly equilibrium free energy profile^{50,82,87}. Among these, the approach proposed by Babin and coworkers⁵⁰ is in our opinion one of the most intuitive and versatile ones, since it allows in a simple way to simultaneously estimate the statistical error and to eliminate systematic errors introduced by the deposition protocol. The basic idea is the following: a metadynamics run is performed up to the build-up time t_b , so that the whole collective variables space has been explored, and the total potential energy – sum of the physical and the bias potential – at the end of the run reads

$$V(x) = U(x) + U_{\text{bias}}[s(x), t_b] \quad . \quad (1)$$

At this point, a molecular dynamics simulation in the potential V is performed, much in the spirit of umbrella sampling, whereas the biasing potential has been determined in an adaptive way by the metadynamics run. The dynamics is characterized by an almost diffusive behavior in the collective variables space, since the meta-stabilities have been removed by the bias potential, provided that all the states of the new potential $V(x)$ are separated by energy barriers comparable or lower than the thermal energy scale $k_B T$. The deviation from a truly diffusive behavior is due by residual features of the free energy landscape which are originated from the statistical and systematic errors in the metadynamics run. During this equilibrium run, the phase space is sampled with probability density

$$\rho_{\text{bias}}(s) = \frac{e^{-\beta\{F(s)+U_{\text{bias}}[s(x),t_b]\}}}{\int ds e^{-\beta\{F(s)+U_{\text{bias}}[s(x),t_b]\}}} \quad (2)$$

that can be estimated by computing the histogram $\rho_{\text{bias}}(s) = (t - t_b)^{-1} \int_{t_b}^t \delta[s - s(t')] dt'$ during the run. Eventually, the free energy profile is given, up to an additive constant, by

$$F(s) = -U_{\text{bias}}[s(x), t_b] - k_B T \ln \rho_{\text{bias}}(s). \quad (3)$$

In the exact expression Eq. 3, the term $k_B T \ln \rho_{\text{bias}}(s)$ can be regarded as a correction to what is the standard metadynamics estimate of the free energy landscape, $F_{\text{meta}}(s) = -U_{\text{bias}}(s)$. This correction term compensates for the systematic errors introduced by the deposition protocol, which are not completely under control in the metadynamics run. In other words, from a simple metadynamics run there is no way to guarantee that the term $\rho_{\text{bias}}(s)$ has become a constant within statistical fluctuations. The corresponding statistical error can be estimated from the fluctuations of $\rho_{\text{bias}}(s)$ using standard error analysis. Differently from the approach involving only a metadynamics run, one should not worry about the speed of

the deposition process (which involves the height, width and deposition rate of the Gaussian functions) as long as the subsequent equilibrium run is ergodic. This means that the Gaussian functions placed during the build-up phase have only to (a) be smaller than $k_B T$, (b) being of width comparable or smaller than the finest detail of the free energy landscape which is *deeper* than $k_B T$ and (c) cover the whole conformational space of the collective variables.

This idea of employing the biasing potential with an umbrella-like sampling has been applied, besides to metadynamics⁵⁰, also to the local elevation method⁴³.

B. Puckering Coordinates

The generalized coordinates introduced by Cremer and Pople^{51,52} can be used to identify puckered conformations of rings with an arbitrary number of members. Their definition makes use of the projections z_j of the position vector of each ring atom onto the axis of the mean ring plane. In the case of six-membered rings they can be defined in terms of the distances z_j as a functions of 3 parameters,

$$q_2 \cos \phi_2 = \sqrt{\frac{1}{3}} \sum_{j=1}^6 z_j \cos \left[\frac{2\pi}{3}(j-1) \right] \quad (4)$$

$$q_2 \sin \phi_2 = -\sqrt{\frac{1}{3}} \sum_{j=1}^6 z_j \sin \left[\frac{2\pi}{3}(j-1) \right] \quad (5)$$

$$q_3 = \sqrt{\frac{1}{6}} \sum_{j=1}^6 (-1)^{j-1} z_j \quad . \quad (6)$$

This coordinate set (q_2, ϕ_2, q_3) can be conveniently expressed as a spherical coordinate set (Q, θ, ϕ) ,

$$\begin{cases} q_2 \cos \phi_2 = Q \sin \theta \cos \phi \\ q_2 \sin \phi_2 = Q \sin \theta \sin \phi \\ q_3 = Q \cos \theta, \end{cases} \quad (7)$$

where $\theta \in [0, \pi]$, $\phi \in [0, 2\pi)$ and Q , the so-called total puckering amplitude, is defined as $Q^2 \equiv \sum_{j=1}^6 z_j^2 = \sum_m q_m^2$.

There are two main interconversion paths in pyranoses, namely, the inversion path — connecting the 4C_1 and 1C_4 conformers — and the pseudo-rotation path⁵¹ — connecting the more flexible boat and skew-boat conformers — that can be easily represented in this

coordinate set. The inversion path develops along the θ coordinate from the ${}^4\text{C}_1$ conformer at $\theta = 0$ to the ${}^1\text{C}_4$ one at $\theta = \pi$, while the pseudo-rotation one develops along ϕ , at $\theta = \pi/2$. Notice that ϕ is a 2π -periodic coordinate, meaning that points at $\phi = 0$ or $\phi = 2\pi$ (at a given value of θ) represent the same conformer. This is not true for θ , which is not periodic.

In this sense, the spherical set (Q, θ, ϕ) has the advantage that only the two angular variables are needed as collective variables in order to perform a proper – that is, ergodic and unbiased – exploration of the puckered conformations space of typical six-membered rings. This is because along the radial direction no meta-stabilities occur, and the radial coordinate Q relaxes fast enough to be ergodic for every reasonable set of potential (that is, when the bond lengths are rigid or quasi-rigid). As we showed in a previous work⁷⁷, not every representation of the Cremer–Pople coordinates is equivalent to the end of being used as collective variables for a conformational search. In particular, any two-dimensional subset of Cremer–Pople coordinates whose functional form involves also biasing forces along the direction of Q might suffer from lack of ergodicity and, therefore, lead to biased sampling⁸⁴. In this work we make only use of the angular variables of the spherical coordinate set as collective variables for the metadynamics run.

Alternative generalized coordinates can be in principle employed to characterize the puckered conformers of six-membered rings, such as the three out-of-plane dihedrals introduced by Strauss and Pickett⁸⁸, or other definitions based on three internal dihedral angles^{89–91}. All these alternative schemes produce good puckering coordinates, in the sense that they allow to uniquely map the complete puckering conformational space. However, in the context of conformational search using accelerated methods, oppositely to Cremer–Pople coordinates, (a) they require the exploration of the complete three-dimensional space, being therefore less convenient than a two dimensional phase space search, and (b) the set of micro-states corresponding to the different conformers generally define less simple surfaces which, as it will be discussed later, might affect the determination of the relative populations of conformers.

C. Simulation Details

The metadynamics and equilibrium simulations have been performed using a version of the GROMETA simulation package^{92–95}, previously modified to allow the usage of the θ and ϕ angular coordinates of Cremer and Pople, as described in Ref. 77. For each of the 16

D-aldopyranoses, a system composed of the respective sugar ring in a cubic simulation box filled with 504 water molecule was set up. The SPC⁹⁶ model has been used to describe the water molecules employed to hydrate each of the pyranoses. The SETTLE algorithm has been used to make water rigid⁹⁷, and all bond lengths in the sugar molecules have been constrained using the SHAKE algorithm⁹⁸. An integration step of 0.2 fs has been used for every phase of the simulations. Before starting each run, a 100 ps long molecular dynamics simulation with no bias has been performed to equilibrate the different sugars in their ⁴C₁ conformer.

The metadynamics part of the run consisted in a 4 ns long simulation, using Gaussian potential functions of height 0.5 kJ/mol and with 0.05 rad for both angular variables, to build up the biasing potential. Gaussian functions have been placed every 200 integration steps. The Nosé–Hoover^{99,100} thermostat and the Parrinello–Rahman¹⁰¹ barostat have been applied to simulate isothermal-isobaric conditions at 300 K and 1 atm using relaxation times of 0.1 and 1.0 ps, respectively. The simulation box edges have been kept orthogonal, and have been rescaled using an isotropic pressure coupling, which controlled the trace of the pressure tensor.

Each metadynamics run has been then followed by a 4 ns long equilibrium molecular dynamics run at the same thermodynamic conditions, using the set of Gaussians placed during the metadynamics to generate the time-independent biasing potential. At a difference with Ref. 50, where the Lagrangian metadynamics with truncated Gaussians has been employed, we make use of the standard direct metadynamics. During this run, the histogram $\rho_{\text{bias}}(\theta, \phi)$ has been collected by sampling configurations every 40 fs on a grid of 60×60 points.

IV. PUCKERING FREE ENERGY OF GLUCOSE

The combined metadynamics–umbrella sampling has been first applied to the calculation of the puckering free energy profile of β -D-Glc, employing the standard GROMOS 45a4 parameter set³⁵. In Fig. 3 we present the free energy profile as a function of the Cremer–Pople angular variables θ and ϕ , showing isolines separated by 10 kJ/mol (upper panel). In order to facilitate the comprehension of the plot, the projection of the free energy profile onto the $\phi = 0$ plane (lower panel) is also provided: the lower contour of the colored region in the projected profile allows to easily identify the minima along the θ coordinate (corresponding

to the minima of this lower contour) and the transition states, or free energy saddle points (corresponding to the maxima of the lower contour). On the (θ, ϕ) plane, ${}^4\text{C}_1$ (0,-), ${}^1\text{C}_4$ (π ,-), and ${}^3,{}^0\text{B}$ ($\pi/2,0$) conformers are clearly recognizable as minima basins. Notice that, due to the periodic nature of ϕ , the ${}^3,{}^0\text{B}$ conformer appears in this representation to be split in two across the $\phi = 0$ line. Another local minimum basin, more shallow than the previous ones is located around the ${}^1\text{S}_3$ ($\pi/2,7\pi/6$) conformer and seems to include also some other near boat-like conformer. This kind of occurrence can be a natural feature for gluco-pyranoses, because of the high flexibility of the ring conformers along the pseudo-rotational path (located at $\theta = \pi/2$). A more detailed description of this local minimum is anyway beyond the interest of this work, because of its very high free energy.

In addition to the free energy profile, in Fig. 4 we show an analogous plot, presented both on the (θ, ϕ) plane (upper panel), and projected onto the $\phi = 0$ plane (lower panel), of the correction to the free energy profile coming from the umbrella sampling phase, $-k_{\text{B}}T \ln \rho_{\text{bias}}(s)$. Performing a screening of this contribution is quite important, because it allows to check if residual meta-stabilities (recognizable as basins) are left after the metadynamics phase, and whether an ergodic sample of the interesting region in the (θ, ϕ) plane has been performed or not: poorly sampled regions will appear wither as peaks. In Fig. 4 it is possible to see that the metadynamics run performed reasonably well. Indeed, the paths connecting the original metastable states do not show residual metastabilities, being the more pronounced minimum, located close to $(0, \pi/3)$, only $\simeq 2$ kJ/mol deep. It is seen that the complete space of puckering angles has been sampled properly. Corrections to the free energy difference between ${}^4\text{C}_1$ and ${}^1\text{C}_4$ are $\simeq 2$ kJ/mol. In case of the next most populated state, ${}^3,{}^0\text{B}$, the correction increases to $\simeq 4$ kJ/mol, while for other states the correction can reach, but never exceeds, $\simeq 6$ kJ/mol with respect to the free energy of ${}^4\text{C}_1$. The umbrella phase thus contributes in a significant way to the estimate of free energy differences, and — as expected — appears to be more important for less populated states and for transition states.

Both the ${}^1\text{C}_4$ and ${}^3,{}^0\text{B}$ puckering free energies (local minima at about 10 and 17 kJ/mol, respectively) appear to be lower than what one would expect. In particular, the free energy of the inverted chair is about 15 kJ/mol lower than both our reference values^{62,63}. This free energy difference leads to a inverted chair population of about 1%, which can be observed during regular molecular dynamics runs at equilibrium. While not strictly incompatible with

NMR experiments, which usually have a resolution of $\simeq 2\%$, this value is certainly strikingly lower than all other theoretical estimates. This fact is even more important if one considers that β -D-Glc is supposed to have the largest 1C_4 free energy among aldopyranoses. It is thus expected that the 1C_4 conformers of the other stereoisomers could be characterized by even lower free energy differences. As it will be discussed in Sec.V, this scenario is only partially correct, as unexpected patterns of the chair–inverted chair free energy difference appear along the series.

While the value of the free energy at the local minima is certainly interesting, a more direct connection with experimentally measurable quantities is performed through the calculation of the population of the basins associated with each of the recognizable conformers. To this aim, the (θ, ϕ) plane has been partitioned in four regions covering the four main basins: $\theta \in [0, \pi/3]$, associated to 4C_1 ; $\theta \in [2\pi/3, \pi]$, associated to 1C_4 ; $\theta \in [\pi/3, 2\pi/3]$ and $\phi \in [-2\pi/3, 2\pi/3]$, associated to 3O_B ; $\theta \in [\pi/3, 2\pi/3]$ and $\phi \in [2\pi/3, 4\pi/3]$, associated to the mixture around 1S_3 . This partitioning of the conformational space appears to be quite natural, since the separating lines are located with good approximation along the maxima of the free energy surface (as is evident especially from the side-view of the free energy landscape, lower panel of Fig. 3) and, therefore, also close to the transition states. The population of a region S can then be calculated simply as

$$p(S) = Z^{-1} \int_S e^{-F(\theta, \phi)/k_B T} d\theta d\phi \quad (8)$$

where the integral of the normalization factor

$$Z = \int e^{-F(\theta, \phi)/k_B T} d\theta d\phi \quad (9)$$

is extended to the whole (θ, ϕ) space. According to this numerical estimate, the ${}^4C_1, {}^1C_4, {}^3O_B$ and 1S_3 conformations account for 98.42, 1.52, 0.0461 and $3.7 \times 10^{-4}\%$ of the total population, respectively.

When the manuscript was in preparation, we discovered that Hansen and Hünenberger already performed an analysis of the puckering free energy of glucose⁴³. To our surprise, their estimates of the inverted chair free energy differ by a non-negligible amount from that presented here, although the same force field and thermodynamic conditions have been used. It has to be noticed that in the approach of Hansen and Hünenberger, free energies are derived from populations by inverting Boltzmann formula. We did the same and obtained a

value of 10.43 kJ/mol for the free energy of 1C_4 , while in Ref. 43 this value ranged from 16.0 to 16.5 kJ/mol (see Tab.4 in Ref.⁴³) The difference between these two approaches is quite important, as it translates to inverted chair populations of $\simeq 1\%$ and $\simeq 0.1\%$ for the results of this work and of Ref.43, respectively.

We give here a tentative explanation of this difference. It has to be noticed that the difference is most probably not related to which set of collective variables (Pickett dihedrals versus Cremer–Pople coordinates) has been used to enhance the sampling, because both represent every slow degree of freedom and allow to span the puckering conformational space in an ergodic way. Systematic errors related to the accelerated dynamics should have been eliminated in both approaches, since both sampling methods provide an unbiased estimate, thanks to the equilibrium sampling.

Among the possible reasons are the use of different algorithms for the simulation of isothermal–isobaric conditions, the different system size, cut-off and long range corrections. Another explanation could be related to the way different states are defined: partitioning the conformational space using the three Pickett angles might lead to a miscounting of states, when using convex shapes like cubes or ellipsoids to perform cuts, as free energy basins in the three-dimensional space of Pickett angles can have more complex, non-convex shape (compare for example Figs 2c and 3c in Ref. 43). By employing Cremer–Pople coordinates only two coordinates, θ and ϕ , need to be taken into account. Performing the appropriate cuts to identify the different states is far a simpler task in two dimensions than in three, also taking into account that only straight cuts along the θ and ϕ directions are needed to identify in a proper way the different basins. Still, more investigation would be needed to address properly this subject, which is out of the scope of this work.

V. PUCKERING FREE ENERGY OF ALDOPYRANOSSES

A. The 45a4 Parameter Set

Apart from the problems related to a correct definition of different puckered states, it is clear that the calculation of the free energy profile of β -D-Glc alone cannot be considered exhaustive nor satisfactorily. The theoretical estimates predict a great variety in the conformational free energies of the 16 stereoisomers of β -D-Glc, and puckering properties have to be

checked separately for each of them. For these reasons we decided to compute in a systematic way the puckering free energy landscape for the whole series of α and β -D-pyranoses.

From the point of view of the force field, the stereoisomers of glucose differ only slightly, namely (a) the order of the two central atoms involved in an improper dihedral interaction at a chiral centre has to be inverted, in order to move a residue from the equatorial to the axial conformation; (b) α anomers are distinguished from β anomers by different torsional interactions on the O5–C1–O1–H1 dihedral, and (c) those sugars having O4 and C6 located on the same side of the ring plane (galactose, talose, gulose, idose) are modeled with different parameters for the O5–C5–C6–O6 and C4–C5–C6–O6 dihedral angles³⁵.

Simulations of the remaining 15 stereoisomers of glucose have been performed using the same protocol employed for β -D-Glc. We summarized the results in Fig. 5 and Tab. III. In Fig. 5 we report the free energy difference between the 1C_4 and 4C_1 conformers of α and β -D-pyranoses modeled using the 45a4 force field, along with the theoretical estimates of of Angyal⁶² and of Vijayalakshmi and coworkers⁶³. Two horizontal dashed lines are also drawn at 0 and 5 kJ/mol (approximately $2k_B T$ at room temperature), highlighting the thresholds below which the inverted chair population becomes greater than the chair one, and below which the inverted chair population becomes noticeable, respectively. In Tab. III, free energy differences and populations for the complete α and β series are listed. Beside those of 1C_4 , the free energy difference and population of the next leading conformer are also reported, as well as the location on the (θ, ϕ) plane (and the closest recognizable conformer) of the first transitions next to 4C_1 . Concerning the population of the leading next conformer, the values reported were calculated on the $\theta \in [\pi/3, 2\pi/3]$ region. This choice takes into account all other local minima present along the equatorial line, but their free energy is always so large (as it has been seen for β -D-Glc), that this approximation doesn't change substantially the population of the next leading conformer.

The differences between the theoretical estimates and the simulation results obtained using the GROMOS 45a4 force field are striking. First of all, none of the 16 sugars investigated presents a chair/inverted chair free energy difference in quantitative agreement with the theory, as differences are usually larger than 5 kJ/mol, and in many cases even larger than 10 kJ/mol. More importantly, many of these values are in marked qualitative disagreement not only with the theoretical results, but also with experimental evidence. In fact, α -D-Glc, α -D-Gal, α -D-Man, β -D-Gal and β -D-Man present an inverted chair free energy which

is lower than 5 kJ/mol (approximately $2 k_B T$ at room temperature). This means that a sensible population of inverted chairs, of the order of 10% is expected at equilibrium, in contrast with no experimental evidence of the occurrence of this conformer. The behavior of -D-Tal is even more pronounced, displaying an inverted chair free energy close to zero or, for the β anomer, even negative. This should have been the case of idose, whose inverted chair conformers have been experimentally detected. On the contrary, the puckering free energy of idose inverted chairs simulated using the 45a4 set of parameters results to be greater than 10 kJ/mol, therefore ruling out the possibility of observing idose inverted chairs in equilibrium simulations.

The GROMOS 45a4 force field appears to be unable not only to compare quantitatively with experimental and theoretical results, but — even more importantly — to reproduce the qualitative behavior of any of the two series. Given the ubiquitous presence of galactose and mannose in relevant oligo and polysaccharides of biological origin, the inability of the force field to prevent appearance of inverted chairs at room temperature seems to be a severe drawback, at least for out-of-equilibrium simulations.

While the free energy of different ring conformers is certainly an important physical quantity, one should not overlook the importance of the kinetics of the conformational transitions. One might reason that alternate conformers might not be seen during equilibrium simulations, if the inverse transition rate is much longer than the typical time interval spanned by a simulation. This pragmatic approach could be hazardous, given the fast pace of increase in simulations sizes and lengths, but nevertheless appealing. Kräutler and coworkers²⁸ reported that in 200 ns long simulation runs of β -D-Glc, β -D-Gal, β -D-Man and β -D-talose, all sugars but glucose remained for more than 99.9% of the time in the chair conformation, while glucose was found in boat and twisted conformation for the 0.7% of the time (giving a rough estimate of the characteristic time of escape from the chair conformer basin of 10 ns).

Although 200 ns is a time much longer than that of most simulations, one should keep in mind that conformational transitions are stochastic events, and a characteristic time of 10 ns might lead to a considerable amount of “unwanted” conformers in simulation runs much shorter than 200 ns, but with more than just one sugar molecule in solution. We tested a setting which we consider to be representative of a typical simulation of medium to large size, namely, of a 25 ns long run at constant temperature and pressure of 512 β -D-Glc and

25×10^3 water molecules in a simulation box with an edge of approximately 9.6 nm, using a cut-off of 1.3 nm for every nonbonded interaction, and an integration timestep of 2 fs. Every other parameter and algorithm employed has been the same as in the metadynamics run discussed so far. Indeed, we observed the appearance of both boats and inverted chairs conformers, with a statistical frequency of 0.06% and 1.1%, respectively (see the upper panel of Fig. 6. These values are close to the one expected from the free energy calculations (see Tab. III). However, a look at the time evolution of the number of inverted chain in the simulation box (lower panel of Fig. 6) tells us that equilibrium has not been reached yet. Still, this result is to our opinion quite valuable, because it gives some information about the kinetics of ring conformational transitions in β -D-Glc, showing that it is not unlikely to observe inverted chair conformers in equilibrium simulations of conventional size, using the 45a4 parameter set.

We performed similar simulations of other sugars, namely, β -D-Gal and α -D-Glc, and in both cases we observed the appearance of inverted chairs, although to a much smaller extent, showing that the kinetics of the chair to inverted chair transition is much slower in these cases (consistently with the results of Ref. 28). This fact is obviously related to the height of the barrier that separates 4C_1 conformers from other ones (see Tab. III), which appears to be lower in β -D-Glc than in all other cases.

B. Force Field Re-parametrization

After realizing the difficulties of the 45a4 parameter set in reproducing puckering properties of pyranoses, we planned to re-parametrize the force field, by finding a minimal set of changes that could fix at least the qualitative aspects discussed so far. At a first glance, this task could seem a bit intimidating, because puckering variables (and therefore the relative free energy landscapes) depend directly on all six ring atoms and also — indirectly, but possibly to a considerable extent — on the ring substituents. The number of parameters on which puckering free energy depends is, therefore, quite high. A completely automated procedure is out of question, and one needs to adopt an heuristic approach.

To keep the re-parametrization as general as possible, and the number of parameters to be tuned low, we decided that our approach should adhere to the following criteria: (a) only parameters not directly involved in inter-molecular interactions should be tuned; (b) the

changes should not be sugar-dependent; (c) the changes have to preserve previously known or already tuned molecular properties; (d) the inverted chair free energy of most common sugars (glucose, galactose, mannose) should be higher than 10 kJ/mol; (e) the trend of the inverted chair free energy as a function of the sugar type, as well as (f) the approximate offset between the inverted chair free energies of α and β anomers, have to be reproduced.

Within this framework, a complete, quantitative agreement for every sugar type is most probably not feasible, especially given the constraints (a) and (b). However, we found that quite reasonable results can be indeed achieved with minimal parameter changes. Point (a) requires Lennard-Jones parameters and partial charges of the 45a4 parameter set to be preserved. Together with the requirement at point (d), this suggests that only angular or torsional interactions involving three or more ring atoms should be the target of our optimization. This is because among the known properties which are well reproduced by the GROMOS 45a4 force field there are the rotameric distribution of the hydroxymethyl group and the conformation of the glycosidic linkages (in di-saccharides). We realized quite soon that changing the stiffness of angular interactions did not change the puckering free energy noticeably. Spieser and coworkers³⁴ showed that the height energetic barrier between 4C_1 and 1C_4 can be increased by stiffening the angular interactions. However, this affects only the free energy of the transition states, and not the free energy difference of the metastable conformers.

Therefore, we concentrated on the torsional interactions, and noticed that every torsional interaction involving three ring atoms (C1,C2,C3,C4,C5 or O5) and either C6 or any hydroxyl oxygen (O1,O2,O3,O4) was either not present (this is the case of O4-C4-C5-O5, C3-C4-C5-C6, O2-C2-C1-O5, C1-O5-C5-C6 and C5-O5-C1-O1) or present with a phase term $\cos(\delta) = +1$ and multiplicity $n = 2$ in the torsional potential

$$U(\phi) = k_\phi [1 + \cos(\delta) \cos(n\phi)], \quad (10)$$

associated to the dihedral angle ϕ . As it was pointed out in Ref. 43, such a phase favors the axial conformation of the substituent, with respect to the equatorial one, whereas a negative value of $\cos(\delta)$ would favor the equatorial conformation with respect to the axial one. Indeed, one of those interactions (O2-C2-C1-O5) has been eliminated in the 45a4 version of the GROMOS force field, for the precise purpose of stabilizing the 4C_1 conformer. While this is true for glucose, it is not, *e.g.*, for mannose, whose substituent in C2 is axial in the chair

conformer. Therefore, the change in the 45a4 set that stabilized the glucose chair, acted in the opposite direction for mannose, stabilizing the inverted chair.

It is clear that any change on these torsional parameters will have a profound (and sugar-specific) effect on the whole series of pyranoses. Therefore, to make grounded changes to the force field, one has first to understand how the pattern of axial and equatorial substituent in the 4C_1 conformer, for given torsional interactions involving the five chiral centres, can influence the properties of the 1C_4 free energy curves of the α and β series.

Firstly, we realized that by changing the sign of $\cos(\delta)$ in the C1–C2–C3–O3 and C5–C4–C3–O3 interactions, one can at the same time rise the 1C_4 free energy of glucose, galactose, mannose, and talose, and lower that of allose, gulose, altrose and idose. Looking at the location along the free energy series of these sugars, it appears that these interactions are leading candidates to recover the approximate monotonous trend in the 1C_4 free energy and, consequently, to fix consequently point (e).

Another important role in determining the shape of the free energy curve is played by a dihedral interaction which is not present in the 45a4 parameter set, namely, the one involving the substituent at the C5 chiral center. The chirality of C5 is the same for all 16 stereoisomers of D-Glc, and can be actually exploited to introduce a global shift for the 1C_4 free energies of the whole series of 16 D-pyranoses. While this gives some freedom in our parametrization process, it should be kept in mind that, most probably, parameters optimized this way are not valid to model the series of L-pyranoses.

In addition to the interactions discussed so far, to reproduce correctly the gap between the 1C_4 free energy curves of the α and β series — as it is apparent, for example, in the theoretical data presented in Fig. 5 — the torsional interaction for the C3–C2–C1–O1 present in the 45a4 set has to be modified. The chirality of the C1 carbon atom differs only between the α and β anomers, and is certainly playing a role in modulating the height of the free energy gap between α and β anomers.

The case of idose is striking, because non-bonded interactions between the substituent in C1 and the other interaction centres are, for this sugar, relatively weak with respect to those of the other substituents. Therefore, the torsional interaction C3–C2–C1–O1 will be the leading actor in determining the gap in free energy between α -D-Ido and β -D-Ido. By performing a simulation with no torsional interaction on C3–C2–C1–O1 for both the α and β anomers of idose, the gap between the 1C_4 free energies, indeed, vanished (within statistical

error bars of 0.4 kJ/mol). This fact could in principle be exploited to fix the C3–C2–C1–O1 interaction so that it reproduces the gap between the $^1\text{C}_4$ free energies of α and β idose. In practice, however, we were unable to proceed along this line, because we did not manage to obtain satisfactorily puckering properties for idose and all other sugars at the same time. This could be related either to the fact that, admittedly, we did not perform a complete exploration of the parameter space due to the high demand of computational resources of this task or, to the fact that also non-bonded interactions should be re-parametrized, given the complex interplay typical of effective force fields. Eventually, some additional corrections were made by adding the same kind of torsional interaction on the dihedral C4–C3–C2–O2, which is related to the position of the substituent at the chiral carbon C2.

In summary, the phase and amplitude of the C3–C2–C1–O1, C4–C3–C2–O2, C1–C2–C3–O3, C5–C4–C3–O3 and C1–O5–C5–C6 torsional interaction were tuned by trial and errors in order to obtain $^1\text{C}_4$ free energy curves in better agreement with experimental and theoretical data. The set of torsional interactions and their parameters for the proposed modification to the 45a4 parameter set are reported in Tab. IV. It is worth mentioning that the strength of the C1–C2–C3–O3 and C5–C4–C3–O3 torsional interactions had to be set to a much higher value (2.4 kJ/mol) than that of the other ones involving three ring atoms and one hydroxyl oxygen. Given the similar chemical nature of the quadruplets of atoms involved (beside that of the anomeric oxygen), such asymmetry appears to be peculiar. This might originate from other interaction terms already present in the 45a4 set, whose influence on the puckering free energy is not yet understood, and that might deserve a separate investigation.

The new parametrization of the GROMOS force field for sugars was performed with the aim not to change properties other than puckering, and dihedral interactions directly involved in the rotameric distribution of the hydroxymethyl group were thus not changed. This choice alone, however, is no guarantee that this quantity is not affected. We checked explicitly that these modifications did not affect the rotameric distribution of the hydroxymethyl group, calculating the free energy profile of the C4–C5–C6–O6 torsional angle for the 45a4 and new sets of parameters. The results obtained with the two parameter sets did not differ more than 2% between each other. The free energy surfaces have been calculated employing the same metadynamics/umbrella sampling approach employed for the calculation of the puckering free energy, but using a Gaussian width of 0.1 rad.

We summarized the results obtained using our modified set of parameters in Figs. 7,8,9

and Tab. V. In Fig. 7 the free energy differences between inverted chair and chair conformers are compared again with the theoretical predictions of Ref. 63 and Ref. 62. The improvement with respect to the results obtained with the 45a4 set (Fig. 5) is striking. Both the α and β series reproduce now the qualitative trend of the theoretical estimates. Galactose, mannose, and talose are not anymore below the $2k_B T$ threshold, and the value of gulose, altrose and idose free energies diminished considerably. Also the gap between the α and β anomers is now reproduced reasonably well, being on average $\simeq 5\text{kJ/mol}$. Noticeably, the height of the free energy barrier of β -D-Glc has been increased considerably, from $\simeq 25\text{kJ/mol}$ to $\simeq 45\text{kJ/mol}$. This increase, which changes dramatically the kinetics of the conformational transition of β -D-Glc, has no counterpart in any other β -anomer. The situation for α -anomers is slightly different, because the height of the free energy barrier close to 4C_1 increased markedly for α -D-Tal and α -D-Gul and, at the same time, decreased for α -D-All and α -D-Alt.

Unfortunately, the population of inverted chairs in α -D-Ido is still lower than that of chairs, whereas both theory and experiment show a preference for the 1C_4 conformer. However, given the fact that these changes are not sugar-specific, the result obtained is to our opinion still remarkable, as the ability to reproduce puckering properties has increased dramatically, with respect to the 45a4 set.

We expect that a more in-depth analysis and parameter fine-tuning could lead to even better agreement with theory and experiments.

VI. CONCLUSIONS

We performed the first systematic calculation of puckering free energy landscapes for the series of α and β -aldohexoses using the latest parameter set (45a4) for the GROMOS force field. While the realism in reproducing the population of inverted chairs and boats for β -D-glucose has surely improved with respect to the 45a3 set, it is still in marked quantitative disagreement (around 10 kJ/mol) with available theoretical models. Besides that, we discovered that the free energy difference between inverted chairs and chairs of other pyranoses modeled using the 45a4 set leaves still much to be desired: galactose, mannose, allose, and α -D-Glc present a sizable population of the inverted chair conformer, which has never been observed experimentally. On the contrary, the population of the inverted chair conformer of idose resulted to be negligible in simulation, whereas theoretical approaches

and experimental results confirm the equilibrium between the two chair conformers of idose in solution.

After analyzing the role that some torsional interactions have in modulating the inverted chair free energy curves for both the α and β series of D-aldopyranoses, we tested a new set of parameters which proved to be quite successful in recovering the trend of the inverted chair free energy for all 16 stereoisomers under study. Our parametrization reproduces free energy differences in accordance to experimental and theoretical data always within 5 kJ/mol, but in most cases within 2.5 kJ/mol, that is, $1k_B T$. A closer agreement with the theoretical model of Angyal⁶² or Vijayalakshmi and coworkers⁶³ is probably not needed, given the uncertainties to which these models are subjected. Indeed, while the theoretical models do not provide any confidence interval, an approximate picture can be made by comparing the theoretical results with experimental data on idose⁶⁷, which roughly fall within a 2-3 kJ/mol interval.

The improvement attained with the introduction of this new parameter set is to our opinion substantial, and reached the goal of reproducing known puckering free energy differences while keeping other properties, such as inter-molecular interactions and the rotameric distribution of the hydroxymethyl group, unchanged. These modifications to the GROMOS force field will allow to perform more realistic simulations of D-aldopyranoses. They represent an certain improvement in the study of carbohydrate equilibrium properties, but will have an even more important impact on the evaluation of out-of-equilibrium properties, such as in the case of simulated AFM pulling experiments.

Still, much has to be done regarding the puckering properties of carbohydrates. In particular, the role of skew conformations — possibly detected in the NMR experiments of Snyder and Serianni⁶⁷ but not significantly present in both the 45a4 and new parameter sets — has to be clarified, and different sugars, such as pyranoses of pentose nature, should be investigated to further test the force field. Eventually, the puckering properties of furanoses should deserve further attention. The GROMOS force field, however, is not the only one which has been found to be problematic in reproducing proper puckering properties, and for many force fields the investigations of ring conformer populations are scarce, if not missing at all. Our hope is that, beside the usefulness related to the specific case of the GROMOS force field parametrization, this work could also serve to attract attention to the importance of the puckering problem in carbohydrate simulations, and to stimulate further investigations.

Acknowledgements

The authors thank E. Chiessi and G. Guella for enlightening discussions, and acknowledge the use of the Wiglaf computer cluster of the Department of Physics of the University of Trento. This work has been partially supported by a PRIN grant from the Italian Ministry of Public Education, University and Scientific Research.

* Electronic address: sega@science.unitn.it

- ¹ B. Hardy and A. Sarko, *J. Comput. Chem.* **14**, 848 (1993).
- ² B. Hardy and A. Sarko, *Polymer* **37**, 1833 (1996).
- ³ A. Almond, A. Brass, and J. Sheehan, *J. Mol. Biol.* **284**, 1425 (1998).
- ⁴ K. Ueda, A. Imamura, and J. Brady, *J. Phys. Chem. A* **102**, 2749 (1998).
- ⁵ P. Venkatarangan and A. Hopfinger, *J. Med. Chem.* **42**, 2169 (1999).
- ⁶ K. Lee, D. Benson, and K. Kuczera, *Biochemistry* **39**, 13737 (2000).
- ⁷ F. Cavalieri, E. Chiessi, M. Paci, G. Paradossi, A. Flaibani, and A. Cesaro, *Macromolecules* **34**, 99 (2001).
- ⁸ K. Naidoo and M. Kuttel, *J. Comput. Chem.* **22**, 445 (2001).
- ⁹ Y. W. Kim and W. Sung, *Phy. Rev. E* **63**, 041910 (2001).
- ¹⁰ F. Momany and J. Willett, *Biopolymers* **63**, 99 (2002).
- ¹¹ G. Paradossi, F. Cavalieri, and E. Chiessi, *Macromolecules* **35**, 6404 (2002).
- ¹² G. Paradossi, E. Chiessi, A. Barbiroli, and D. Fessas, *Biomacromolecules* **3**, 498 (2002).
- ¹³ L. Lawtrakul, H. Viernstein, and P. Wolschann, *Int. J. Pharm.* **256**, 33 (2003).
- ¹⁴ M. Umemura, Y. Yuguchi, and T. Hirotsu, *J. Phys. Chem. A* **108**, 7063 (2004).
- ¹⁵ H. Verli and J. Guimarães, *Carbohydr. Res.* **339**, 281 (2004).
- ¹⁶ H. Yu, M. Amann, T. Hansson, J. Köhler, G. Wich, and W. van Gunsteren, *Carbohydr. Res.* **339**, 1697 (2004).
- ¹⁷ C. Sandoval, C. Castro, L. Gargallo, D. Radic, and J. Freire, *Polymer* **46**, 10437 (2005).
- ¹⁸ Y. Xie and A. Soh, *Mater. Lett.* **59**, 971 (2005).
- ¹⁹ J. González-Outeiriño, R. Kadirvelraj, and R. Woods, *Carbohydr. Res.* **340**, 1007 (2005).
- ²⁰ A. Palleschi, G. Bocchinfuso, T. Coviello, and F. Alhaique, *Carbohydr. Res.* **340**, 2154 (2005).
- ²¹ I. Neelov, D. Adolf, T. McLeish, and E. Paci, *Biophys. J.* **91**, 3579 (2006).
- ²² T. Mamonova and M. Kurnikova, *J. Phys. Chem. B* **110**, 25091 (2006).
- ²³ A. Figueiras, J. Sarraguça, R. Carvalho, A. Pais, and F. Veiga, *Pharm. Res.* **24**, 377 (2007).
- ²⁴ D. Kony, W. Damm, S. Stoll, W. van Gunsteren, and P. Hünenberger, *Biophys. J.* **93**, 442 (2007).

- ²⁵ Y. Yoshida, A. Isogai, and Y. Tsujii, *Cellulose* **15**, 651 (2008).
- ²⁶ M. Almlöf, E. Kristensen, H. Siegbahn, and J. Åqvist, *Biomaterials* **29**, 4463 (2008).
- ²⁷ M. Umemura and Y. Yuguchi, *Cellulose* **16**, 361 (2009).
- ²⁸ V. Krautler, M. Muller, and P. Hunenberger, *Carbohydr. Res.* **342**, 2097 (2007).
- ²⁹ S. Perez, A. Imberty, S. Engelsens, J. Gruza, K. Mazeau, J. Jimenez-Barbero, A. Poveda, J. Espinosa, B. van Eyck, G. Johnson, A. D. French, M. L. C. E. Kouwijzer, P. D. J. Grootenuis, A. Bernardi, L. Raimondi, H. Senderowitz, V. Durier, G. Vergoten, and K. Rasmussen, *Carbohydr. Res.* **314**, 141 (1998).
- ³⁰ J. Behler, D. Price, and M. Drew, *Phys. Chem. Chem. Phys.* **3**, 588 (2001).
- ³¹ F. Corzana, M. Motawia, C. Hervé Du Penhoat, S. Perez, S. Tschampel, R. J. Woods, and S. Engelsens, *J. Comput. Chem.* **25**, 573 (2004).
- ³² L. Kroon-Batenburg, P. Kruiskamp, J. Vliegenthart, and J. Kroon, *J. Phys. Chem. B* **101**, 8454 (1997).
- ³³ J. W. Brady, *J. Am. Chem. Soc.* **108**, 8153 (1986).
- ³⁴ S. A. H. Spieser, J. A. van Kuik, L. M. J. Kroon-Batenburg, and J. Kroon, *Carbohydr. Res.* **322**, 264 (1999).
- ³⁵ R. Lins and P. Hünenberger, *J. Comput. Chem.* **26**, 1400 (2005).
- ³⁶ E. Chiessi, private communication.
- ³⁷ H. Limbach and J. Ubbink, *Soft Matter* **4**, 1887 (2008).
- ³⁸ J. E. H. Koehler, W. Saenger, and W. F. van Gunsteren, *Eur. Biophys. J.* **15**, 197 (1987).
- ³⁹ W. F. van Gunsteren, S. R. Billeter, A. A. Eising, P. Hünenberger, P. Krüger, A. E. Mark, W. R. P. Scott, and I. G. Tironi, *The GROMOS96 Manual and User Guide*, Zürich, Switzerland, 1996.
- ⁴⁰ M. L. C. E. Kouwijzer and P. D. J. Grootenuis, *J. Phys. Chem.* **99**, 13426 (1995).
- ⁴¹ K.-H. Ott and B. Meyer, *J. Com. Chem.* **17**, 1068 (1996).
- ⁴² W. Damm, A. Frontera, J. Tirado-Rives, and W. Jorgensen, *J. Comput. Chem.* **18**, 1955 (1997).
- ⁴³ H. S. Hansen and P. H. Hünenberger, *J. Comput. Chem.* **31**, 1 (2010).
- ⁴⁴ G. Lee, W. Nowak, J. Jaroniec, Q. Zhang, and P. Marszalek, *Biophys. J.* **87**, 1456 (2004).
- ⁴⁵ B. Heymann and H. Grubmüller, *Chem. Phys. Lett.* **305**, 202 (1999).

- ⁴⁶ W. D. Cornell, P. Cieplak, C. I. Bayly, I. R. Gould, K. M. Merz, D. M. Ferguson, D. C. Spellmeyer, T. Fox, J. W. Caldwell, and P. A. Kollman, *J. Am. Chem. Soc.* **117**, 5179 (1995).
- ⁴⁷ R. J. Woods, R. A. Dwek, C. J. Edge, and B. Fraserreid, *J. Phys. Chem.* **99**, 3832 (1995).
- ⁴⁸ R. Eklund and G. Widmalm, *Carbohydr. Res.* **338**, 393 (2003).
- ⁴⁹ J. Gruza, J. Koca, S. Perez, and A. Imberty, *J. Mol. Struct.: THEOCHEM* **424**, 269 (1998).
- ⁵⁰ V. Babin, C. Roland, T. A. Darden, and C. Sagui, *J. Chem. Phys.* **125**, 204909 (2006).
- ⁵¹ D. Cremer and J. A. Pople, *J. Am. Chem. Soc.* **97**, 1354 (1975).
- ⁵² D. Cremer, *J. Phys. Chem.* **94**, 5502 (1990).
- ⁵³ A. McNaught, *Adv. Carbohydr. Chem. Biochem.* **52**, 43 (1997).
- ⁵⁴ S. Rings, *Eur. J. Biochem.* **100**, 295 (1980).
- ⁵⁵ H. Sachse, *Ber. Dtsch. Chem. Ges.* **23**, 1363 (1890).
- ⁵⁶ H. Sachse, *Z. Phys. Chem.* **10**, 203 (1892).
- ⁵⁷ O. L. Sponsler and W. H. Dore, in *Fourth Colloid Symposium Monograph*, p. 174, Chemical Catalog Company, New York, 1926.
- ⁵⁸ V. S. R. Rao, P. K. Qasba, P. Balaji, and R. Chandrasekaran, *Conformation of Carbohydrates*, Harwood Academic Publisher, Amsterdam, 1998.
- ⁵⁹ R. Reeves, *J. Am. Chem. Soc.* **72**, 1499 (1950).
- ⁶⁰ R. Reeves, *Adv. Carbohydr. Chem.* **6**, 107 (1951).
- ⁶¹ R. Kelly, *Canad. J. Chem.* **35**, 149 (1957).
- ⁶² S. Angyal, *Angew. Chem., Int. Ed.* **8**, 157 (1969).
- ⁶³ K. Vijayalakshmi and V. Rao, *Carbohydr. Res.* **22**, 413 (1972).
- ⁶⁴ D. Barton, *Science* **169**, 539 (1970).
- ⁶⁵ Y. Zhu, J. Zajicek, and A. Serianni, *J. Org. Chem.* **66**, 6244 (2001).
- ⁶⁶ F. Franks, P. Lillford, and G. Robinson, *J. Chem. Soc. Faraday. Trans.* **85**, 2417 (1989).
- ⁶⁷ J. Snyder and A. Serianni, *J. Org. Chem.* **51**, 2694 (1986).
- ⁶⁸ S. Immel, K. Fujita, and F. Lichtenthaler, *Chem. Eur. J.* **5**, 3185 (1999).
- ⁶⁹ B. Hakkarainen, K. Fujita, S. Immel, L. Kenne, and C. Sandström, *Carbohydr. Res.* **340**, 1539 (2005).
- ⁷⁰ G. Guella, E. Autieri, and M. Segà, manuscript in preparation., 2010.
- ⁷¹ P. Marszalek, H. Li, A. Oberhauser, and J. Fernandez, *Proc. Natl. Acad. Sci. USA* **99**, 4278 (2002).

- ⁷² Q. Zhang, G. Lee, and P. Marszalek, *J. Phys.: Condens. Matter* **17**, S1427 (2005).
- ⁷³ P. Marszalek, A. Oberhauser, Y. Pang, and J. Fernandez, *Nature* **396**, 661 (1998).
- ⁷⁴ H. Li, M. Rief, F. Oesterhelt, H. Gaub, X. Zhang, and J. Shen, *Chem. Phys. Lett.* **305**, 197 (1999).
- ⁷⁵ M. Kuttel and K. Naidoo, *J. Am. Chem. Soc.* **127**, 12 (2005).
- ⁷⁶ X. Biarnes, A. Ardevol, A. Planas, C. Rovira, A. Laio, and M. Parrinello, *J. Am. Chem. Soc.* **129**, 10686 (2007).
- ⁷⁷ M. Sega, E. Autieri, and F. Pederiva, *J. Chem. Phys.* **130**, 225102 (2009).
- ⁷⁸ S. Barrows, F. Dulles, C. Cramer, A. French, and D. Truhlar, *Carbohydr. Res.* **276**, 219 (1995).
- ⁷⁹ M. Appell, G. Strati, J. Willett, and F. Momany, *Carbohydr. Res.* **339**, 537 (2004).
- ⁸⁰ A. Laio and M. Parrinello, *Proc. Natl. Acad. Sci. USA* **99**, 12562 (2002).
- ⁸¹ M. Iannuzzi, A. Laio, and M. Parrinello, *Phys. Rev. Lett.* **90**, 238302 (2003).
- ⁸² A. Laio, A. Rodriguez-Fortea, F. Gervasio, M. Ceccarelli, and M. Parrinello, *J. Phys. Chem. B* **109**, 6714 (2005).
- ⁸³ G. Bussi, A. Laio, and M. Parrinello, *Phys. Rev. Lett.* **96**, 90601 (2006).
- ⁸⁴ A. Laio and F. L. Gervasio, *Rep. Prog. Phys.* **71**, 126601 (2008).
- ⁸⁵ T. Huber, A. Torda, and W. F. van Gunsteren, *J. Comput.-Aided Mol. Des.* **8**, 695 (1994).
- ⁸⁶ M. Mezei, *J. Comput. Phys.* **68**, 237 (1987).
- ⁸⁷ M. Bonomi, A. Barducci, and M. Parrinello, *J. Comput. Chem.* (2009).
- ⁸⁸ H. L. Strauss and H. M. Pickett, *J. Am. Chem. Soc.* **92**, 7281 (1970).
- ⁸⁹ N. Zefirov, V. Palyulin, E. Dashevskaya, P. XXXIII, I. Mursakulov, V. Svyatkin, and V. Samoshin, *J. Phys. Org. Chem.* **3**, 147 (1990).
- ⁹⁰ C. Haasnoot, *J. Am. Chem. Soc.* **114**, 882 (1992).
- ⁹¹ A. Bérces, D. Whitfield, and T. Nukada, *Tetrahedron* **57**, 477 (2001).
- ⁹² C. Camilloni, D. Provasi, G. Tiana, and R. A. Brogna, *Proteins* **71**, 1647 (2008).
- ⁹³ H. J. C. Berendsen, D. van der Spoel, and R. van Drunen, *Comput. Phys. Comm.* **91**, 43 (1995).
- ⁹⁴ E. Lindahl, B. Hess, and D. van der Spoel, *J. Mol. Mod.* **7**, 306 (2001).
- ⁹⁵ D. van der Spoel, E. Lindahl, B. Hess, G. Groenhof, A. E. Mark, and H. J. C. Berendsen, *J. Comput. Chem.* **26**, 1701 (2005).

- ⁹⁶ H. J. C. Berendsen, J. P. M. Postma, A. DiNola, and J. R. Haak, *J. Chem. Phys.* **81**, 3684 (1984).
- ⁹⁷ S. Miyamoto and P. A. Kollman, *J. Comput. Chem.* **13**, 952 (1992).
- ⁹⁸ J. Ryckaert, G. Ciccotti, and H. Berendsen, *J. Comput. Phys.* **23**, 327 (1977).
- ⁹⁹ S. Nosé, *Mol. Phys.* **52**, 255 (1984).
- ¹⁰⁰ W. Hoover, *Phys. Rev. A* **31**, 1695 (1985).
- ¹⁰¹ M. Parrinello and A. Rahman, *J. Appl. Phys.* **52**, 7182 (1981).

List of Figures

1	Numbering scheme for aldopyranoses rings.	33
2	Different ring shapes for stable ring conformers: chairs (left); boats (center); skews (right).	34
3	Puckering free energy landscape (already corrected with the results from the umbrella sampling phase) of β -D-Glc using the standard 45a4 parameter set. Upper panel: the (θ, ϕ) plane is shown, with isolines drawn every 10 kJ/mol starting from the absolute minimum. Lower panel: projection of the free en- ergy profile onto the $\phi = 0$ plane. Darker colors correspond to lower energies. .	35
4	Contribution to the total puckering free energy of β -D-Glc (45a4 parameters) from the equilibrium sampling, $-k_B T \ln \rho_{\text{bias}}(\theta, \phi)$. An immaterial constant has been added, so that the correction term is zero at the position of the free energy global minimum. Isolines are drawn every 2.5 kJ/mol (upper panel). The projection onto the $\phi = 0$ plane of the correction term (lower panel).	36
5	Inverted chair free energy difference for the β (upper panel) and α (lower panel) series of aldopyranoses. The three curves refer to the simulation results obtained using the 45a4 parameter set (squares) and the predictions of Ref. 62 (triangles) and Ref. 63 (circles). Lines are a guide to the eye, and error bars are always smaller than the symbols (0.5 kJ/mol).	37
6	Results of the unbiased molecular dynamics simulation of β -D-Glc. Histogram of the population along the θ puckering coordinate (upper panel) and time evolution of the number of inverted chairs (lower panel).	38
7	Inverted chair free energy difference for the β (upper panel) and α (lower panel) series of aldopyranoses. The three curves refer to the simulation re- sults using the new parameter set (squares) and the predictions of Ref. 62 (triangles) and Ref. 63 (circles). Lines are a guide to the eye, and error bars are always smaller than the symbols (0.5 kJ/mol).	39
8	Puckering free energy landscapes (in kJ/mol) obtained by the combined meta- dynamics – umbrella sampling, for the series of β -D-aldopyranoses simulated using the new force field parameters. Isolines are drawn every 10 kJ/mol, starting from the global minimum.	40

9	Puckering free energy landscapes (in kJ/mol) obtained by the combined meta- dynamics – umbrella sampling, for the series of α -D-aldopyranoses simulated using the new force field parameters. Isolines are drawn every 10 kJ/mol, starting from the global minimum.	41
---	--	----

Figures

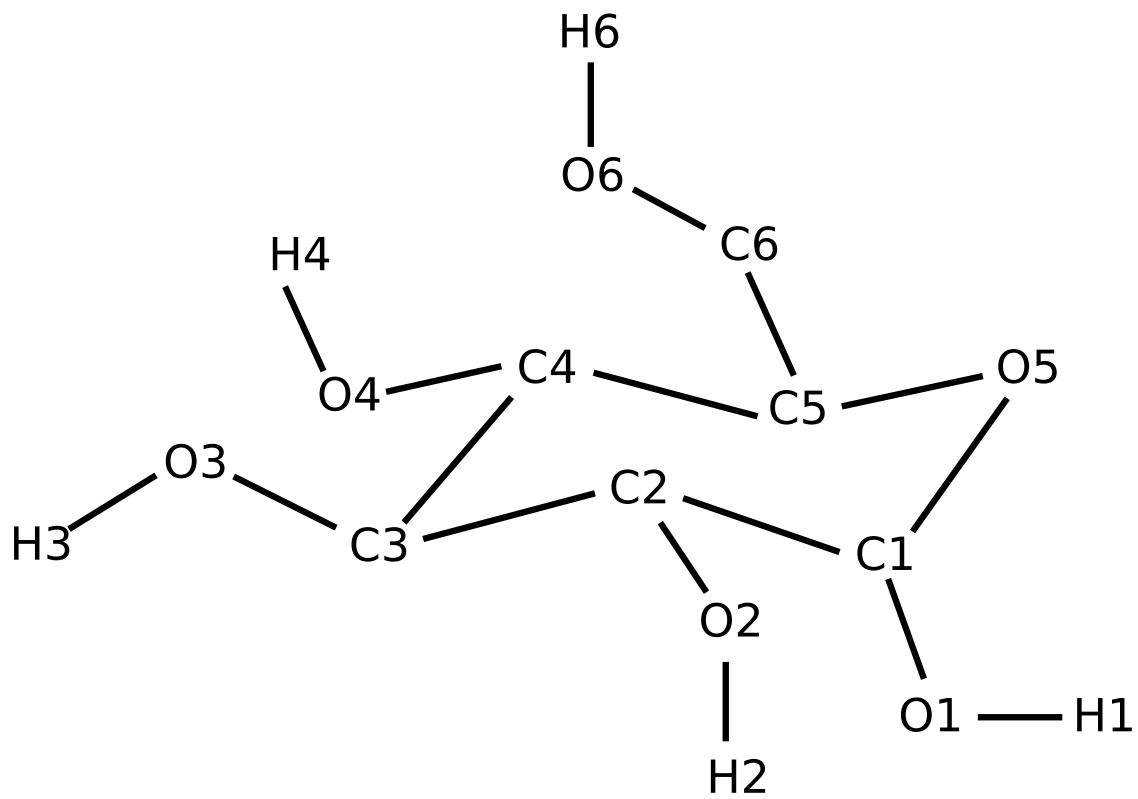


FIG. 1: Numbering scheme for aldopyranoses rings.

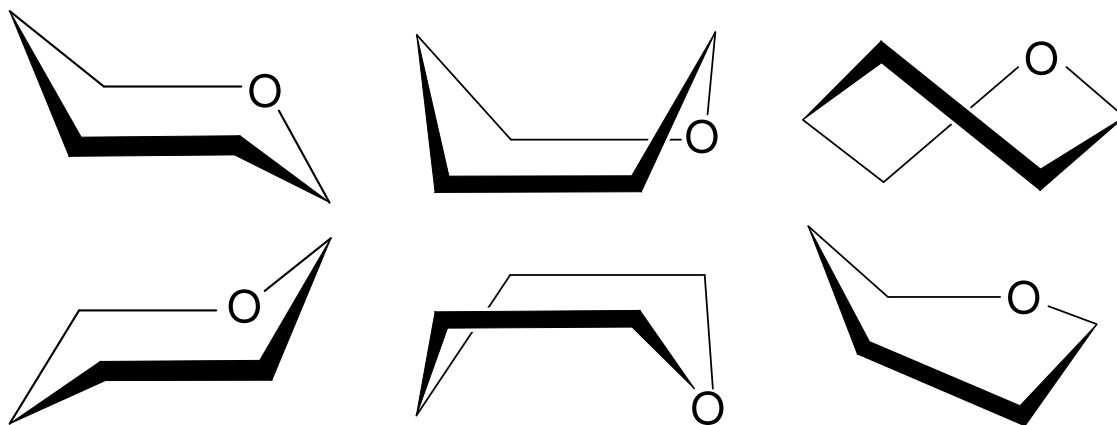


FIG. 2: Different ring shapes for stable ring conformers: chairs (left); boats (center); skews (right).

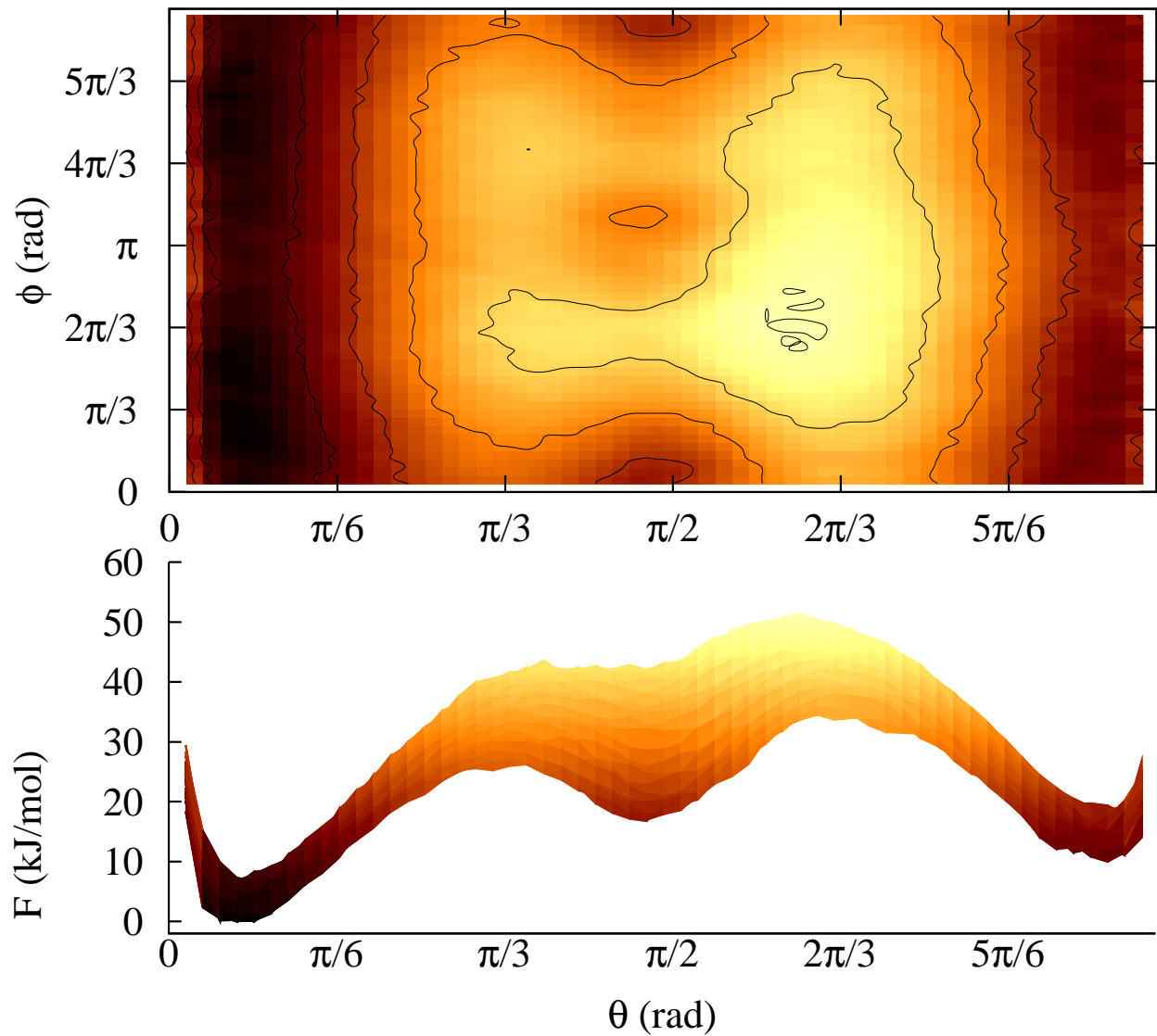


FIG. 3: Puckering free energy landscape (already corrected with the results from the umbrella sampling phase) of β -D-Glc using the standard 45a4 parameter set. Upper panel: the (θ, ϕ) plane is shown, with isolines drawn every 10 kJ/mol starting from the absolute minimum. Lower panel: projection of the free energy profile onto the $\phi = 0$ plane. Darker colors correspond to lower energies.

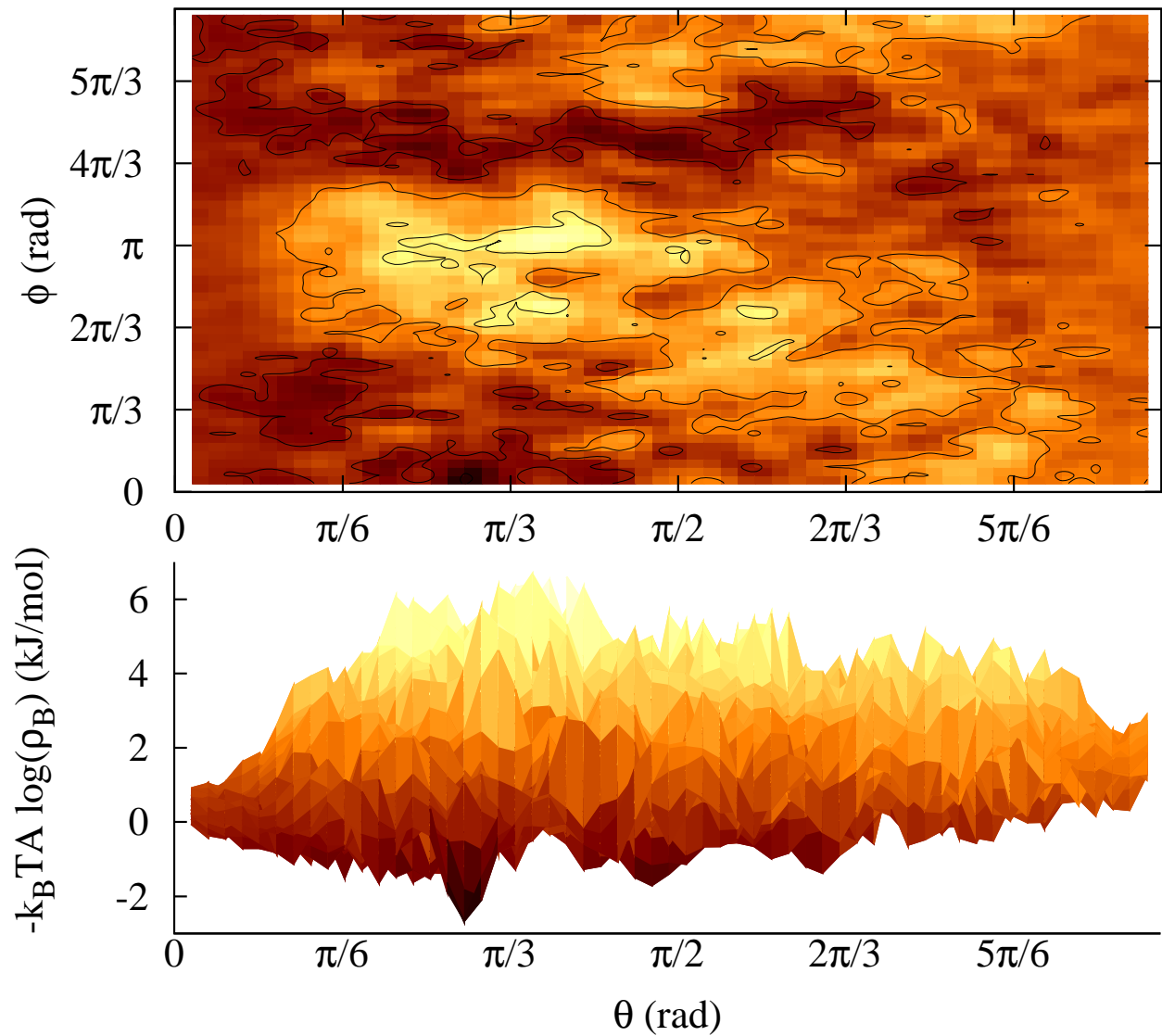


FIG. 4: Contribution to the total puckering free energy of β -D-Glc (45a4 parameters) from the equilibrium sampling, $-k_B T \ln \rho_{\text{bias}}(\theta, \phi)$. An immaterial constant has been added, so that the correction term is zero at the position of the free energy global minimum. Isolines are drawn every 2.5 kJ/mol (upper panel). The projection onto the $\phi = 0$ plane of the correction term (lower panel).

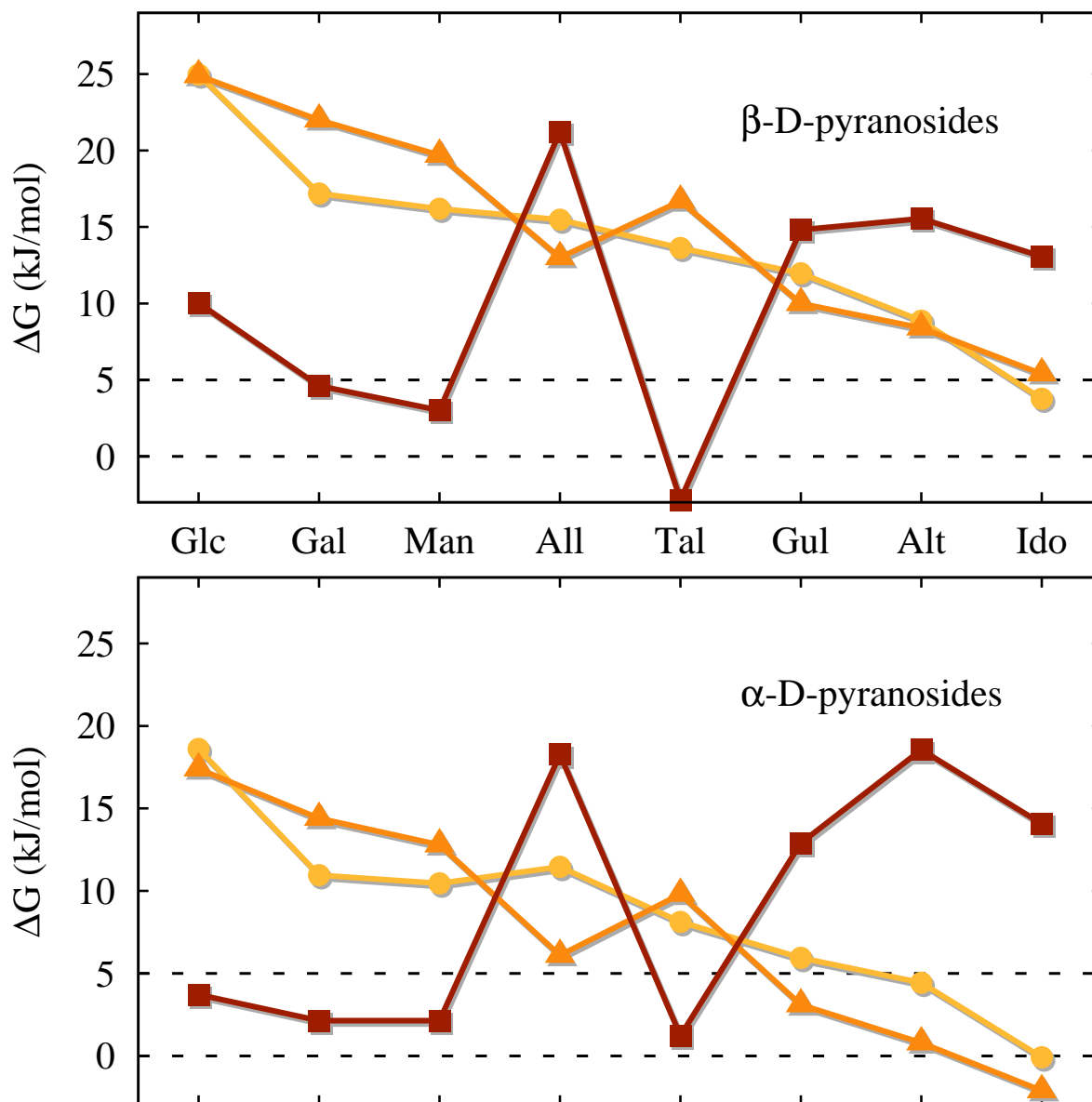


FIG. 5: Inverted chair free energy difference for the β (upper panel) and α (lower panel) series of aldopyranoses. The three curves refer to the simulation results obtained using the 45a4 parameter set (squares) and the predictions of Ref. 62 (triangles) and Ref. 63 (circles). Lines are a guide to the eye, and error bars are always smaller than the symbols (0.5 kJ/mol).

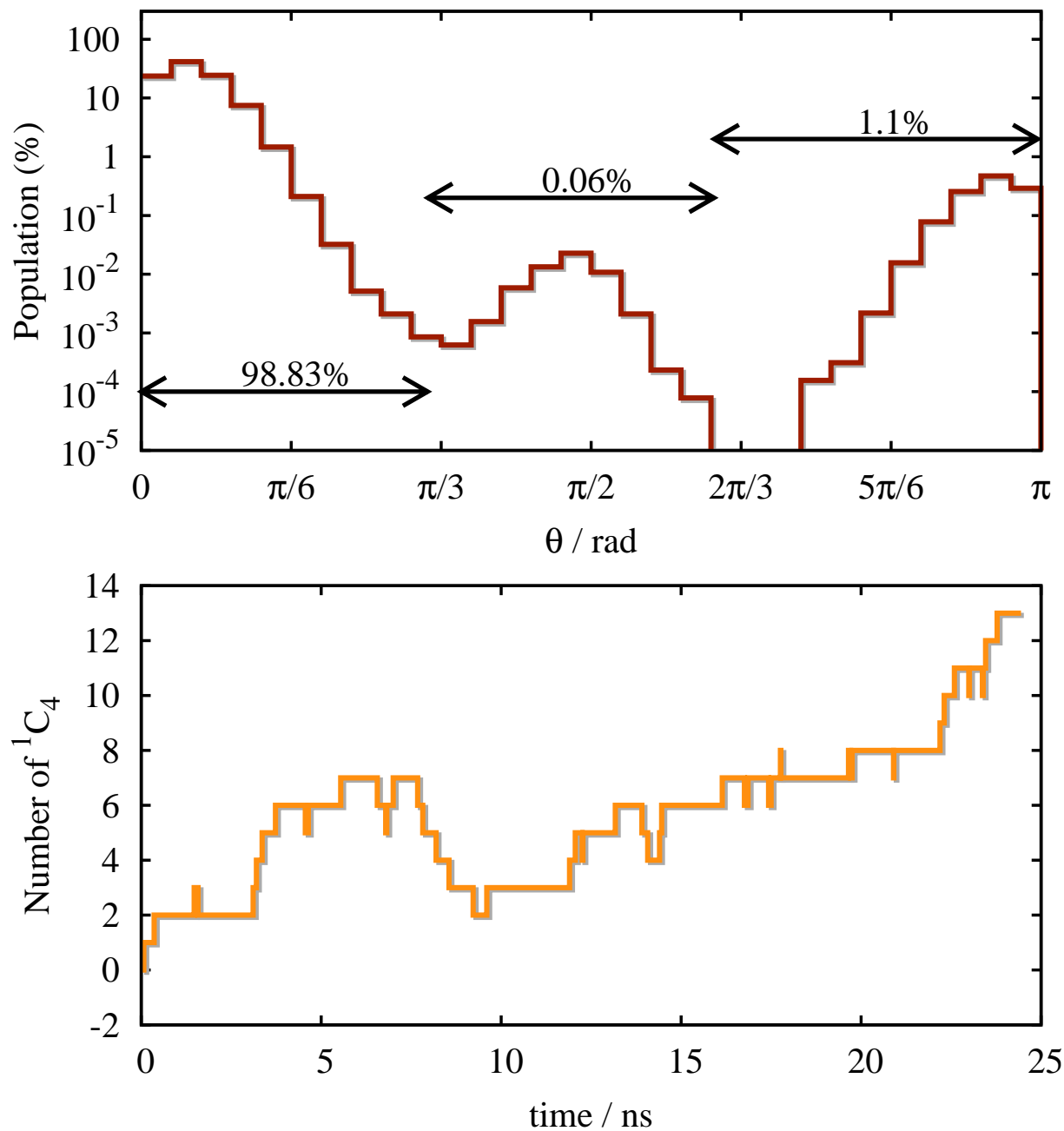


FIG. 6: Results of the unbiased molecular dynamics simulation of β -D-Glc. Histogram of the population along the θ puckering coordinate (upper panel) and time evolution of the number of inverted chairs (lower panel).

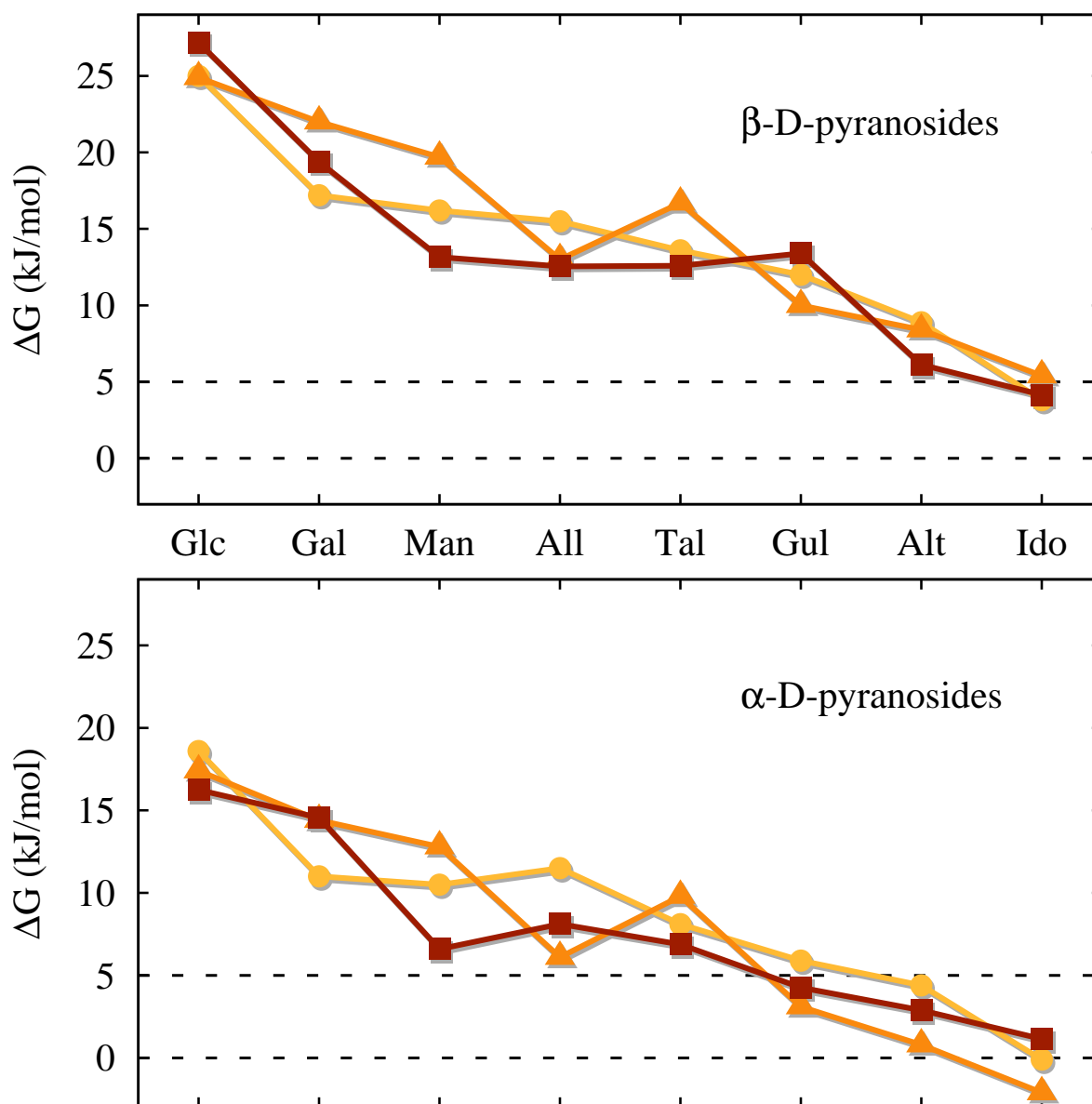


FIG. 7: Inverted chair free energy difference for the β (upper panel) and α (lower panel) series of aldopyranoses. The three curves refer to the simulation results using the new parameter set (squares) and the predictions of Ref. 62 (triangles) and Ref. 63 (circles). Lines are a guide to the eye, and error bars are always smaller than the symbols (0.5 kJ/mol).

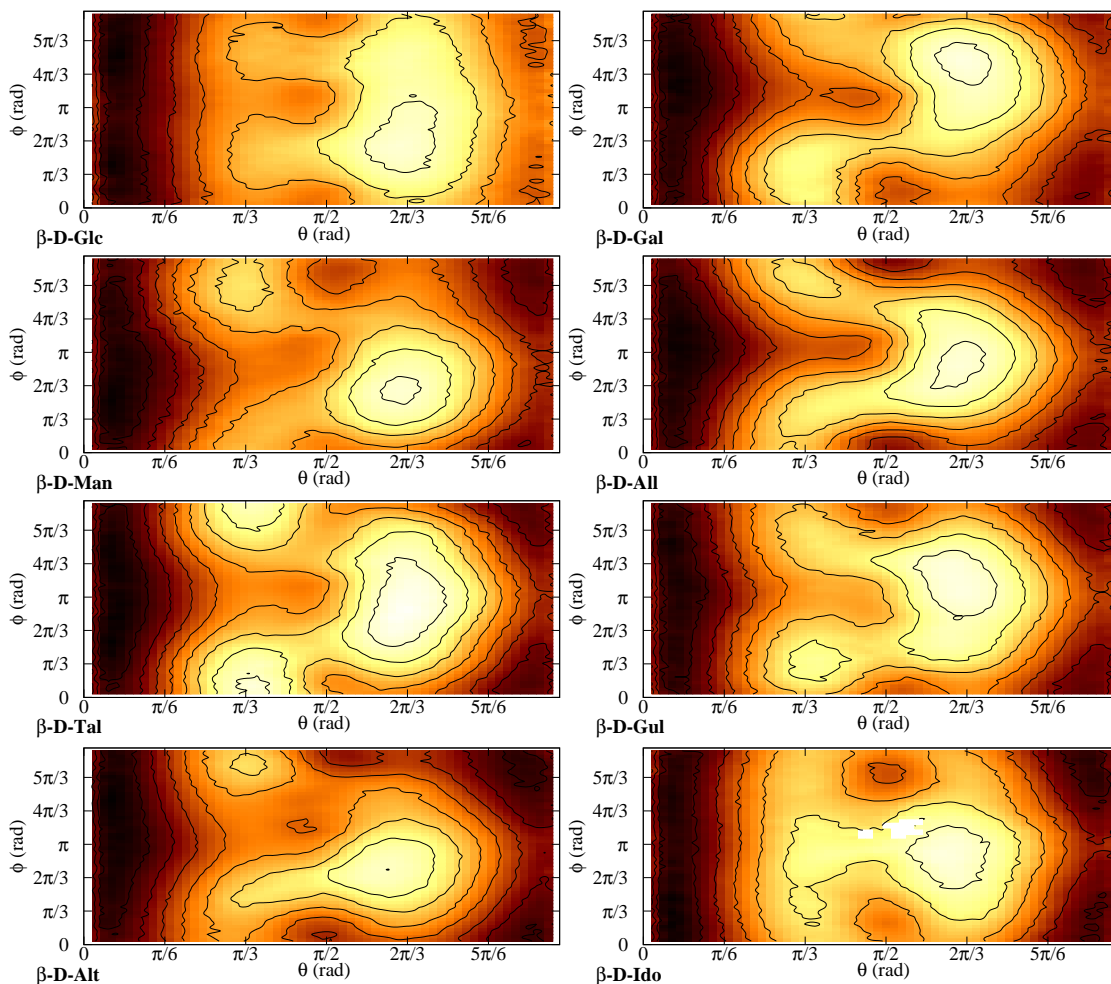


FIG. 8: Puckering free energy landscapes (in kJ/mol) obtained by the combined metadynamics – umbrella sampling, for the series of β -D-aldopyranoses simulated using the new force field parameters. Isolines are drawn every 10 kJ/mol, starting from the global minimum.

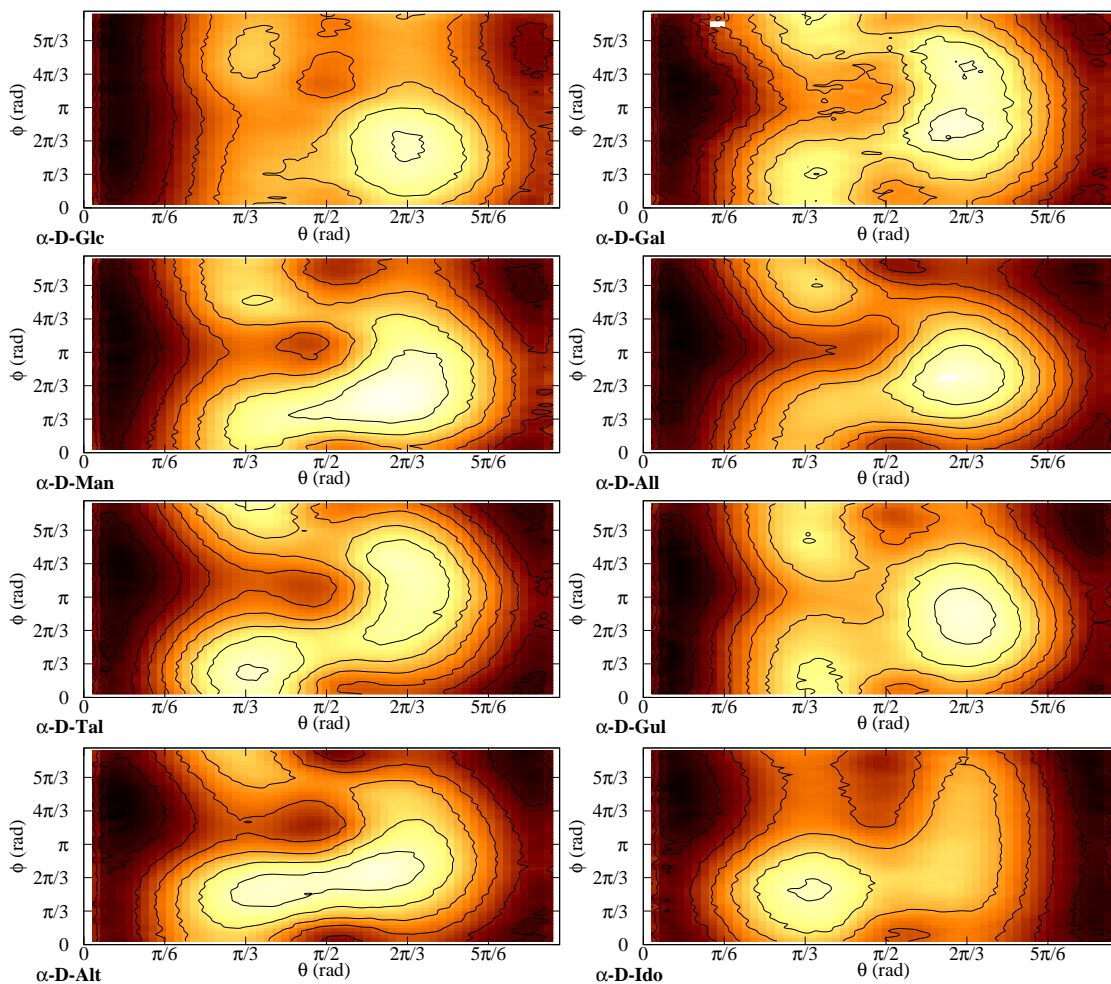


FIG. 9: Puckering free energy landscapes (in kJ/mol) obtained by the combined metadynamics – umbrella sampling, for the series of α -D-aldopyranoses simulated using the new force field parameters. Isolines are drawn every 10 kJ/mol, starting from the global minimum.

Tables

Stereoisomer	C1	C2	C3	C4	C5
β -D-Glc	eq	eq	eq	eq	eq
β -D-Gal	eq	eq	eq	ax	eq
β -D-Man	eq	ax	eq	eq	eq
β -D-All	eq	eq	ax	eq	eq
β -D-Tal	eq	ax	eq	ax	eq
β -D-Gul	eq	eq	ax	ax	eq
β -D-Alt	eq	ax	ax	eq	eq
β -D-Ido	eq	ax	ax	ax	eq

TABLE I: Orientation of ring substituents (ax: axial; eq: equatorial) for different stereoisomers (referred to the 4C_1 conformer).

Method	$\Delta G[\alpha]^b$	$\Delta G[\beta]^b$
Molecular mechanical [†]	-0.08	3.77
Semiempirical [‡]	-2.09	5.43
NMR [§]	-4.0	3.4

^a Free energy of the α -anomer (kJ/mol); ^b Free energy of the β -anomer (kJ/mol); [†] Ref. 63 ; [‡] Ref. 62 ; [§] Ref. 67. A positive value of the difference denotes the 4C_1 as the most stable conformer

TABLE II: Theoretical and experimental estimates of idose inverted chair free energy.

Isomer	ΔG [1C_4] ^a	Next ^b	ΔG [Next] ^c	TS ^d	ΔG [TS] ^e	P[4C_1] ^f	P[1C_4] ^g	P[Next] ^h
β -D-Glc	10.0 ± 0.2	3O_B	16.7 ± 0.2	(1.06,0.10)	25.9 ± 0.2	98.42(1)	1.52(1)	$4.6(1) \times 10^{-2}$
β -D-Gal	4.6 ± 0.2	3S_1	21.5 ± 0.2	(1.11,3.94)	38.6 ± 0.4	91.2(1)	8.8(1)	$6.2(1) \times 10^{-3}$
β -D-Man	3.0 ± 0.2	${}^O S_2$	23.2 ± 0.2	(1.11,2.44)	41.2 ± 0.2	80.6(1)	19.4(1)	$4.3(1) \times 10^{-3}$
β -D-All	21.2 ± 0.2	3O_B	27.9 ± 0.2	(1.17,3.40)	36.9 ± 0.3	99.98(1)	0.0205(2)	$4.6(1) \times 10^{-4}$
β -D-Tal	-2.8 ± 0.2	3O_B	36.8 ± 0.2	(1.11,3.62)	47.6 ± 0.2	58.7(2)	41.3(1)	$3.8(1) \times 10^{-5}$
β -D-Gul	14.8 ± 0.3	${}^O S_2$	33.9 ± 0.1	(1.22,3.30)	43.2 ± 0.2	99.92(1)	0.08(1)	$5.7(1) \times 10^{-5}$
β -D-Alt	15.5 ± 0.2	${}^O S_2$	33.7 ± 0.1	(1.11,3.94)	42.4 ± 0.2	99.87(1)	0.129(2)	$9.4(1) \times 10^{-5}$
β -D-Ido	13.0 ± 0.2	B_{25}	35.0 ± 0.3	(1.06,4.47)	44.9 ± 0.1	99.59(1)	0.412(4)	$6.1(1) \times 10^{-5}$
α -D-Glc	3.7 ± 0.2	${}^O S_2$	25.7 ± 0.2	(1.11,0.21)	35.2 ± 0.2	90.85(6)	9.15(7)	$1.7(1) \times 10^{-3}$
α -D-Gal	2.1 ± 0.2	3S_1	33.0 ± 0.2	(1.11,3.40)	47.1 ± 0.2	74.9(2)	25.1(2)	$5.8(1) \times 10^{-5}$
α -D-Man	2.3 ± 0.3	${}^O S_2$	15.2 ± 0.3	(1.11,3.30)	29.5 ± 0.4	71.9(3)	28.0(2)	$3.9(1) \times 10^{-2}$
α -D-All	18.2 ± 0.2	3O_B	35.6 ± 0.2	(1.65,4.79)	56.6 ± 0.3	99.94(1)	0.060(1)	$3.4(1) \times 10^{-5}$
α -D-Tal	1.2 ± 0.3	1S_3	32.1 ± 0.3	(1.11,3.51)	37.1 ± 0.3	63.7(4)	36.3(3)	$3.0(1) \times 10^{-4}$
α -D-Gul	12.9 ± 0.2	${}^O S_2$	42.7 ± 0.2	(1.06,3.72)	30.5 ± 0.2	99.49(1)	0.51(1)	$7.0(1) \times 10^{-6}$
α -D-Alt	18.5 ± 0.4	${}^O S_2$	23.1 ± 0.2	(1.17,2.87)	45.5 ± 0.3	99.93(1)	0.065(1)	$5.5(1) \times 10^{-3}$
α -D-Ido	14.0 ± 0.2	1S_3	27.9 ± 0.2	(1.11,4.36)	33.6 ± 0.2	99.47(1)	0.524(3)	$1.4(1) \times 10^{-3}$

Energies are expressed in kJ/mol, and probabilities in percent; ^a Free energy of 1C_4 ; ^b Next most

populated conformer after 4C_1 and 1C_4 ; ^c Free energy of the next most populated conformer; ^d Location of the transition state (θ, ϕ); ^e Free energy of the transition state; ^f Population of 4C_1 (%); ^g Population of 1C_4 (%); ^h Population of the next most populated conformer. When a basin is present, which encompasses many states, all conformers involved are listed.

TABLE III: Free energy and population of different conformers using the 45a4 parameter set.

dihedral angle	k_ϕ [§]	$\cos \delta$	n
C3–C2–C1–O1 [†]	0.5	–1	2
C4–C3–C2–O2 [†]	0.5	–1	2
C1–C2–C3–O3 [†]	2.4	–1	2
C5–C4–C3–O3 [†]	2.4	–1	2
C1–O5–C5–C6 [‡]	0.5	–1	2

[§] in kJ/mol; [†] interaction modified with respect to the correspondent 45a4 one; [‡] new interaction term (not present in 45a4); The functional form for the torsional interaction is that of Eq.10. All other interactions are the same as in the 45a4 set³⁵.

TABLE IV: New parameters for D-aldopyranoses torsional interactions.

Isomer	ΔG [1C_4] ^a	Next ^b	ΔG [Next] ^c	TS ^d	ΔG [TS] ^e	P[4C_1] ^f	P[1C_4] ^g	P[Next] ^h
β -D-Glc	27.1 ± 0.3	3O_B	30.9 ± 0.2	(1.17,3.19)	45.9 ± 0.5	99.99(1)	0.002(1)	$4.17(4) \times 10^{-4}$
β -D-Gal	19.3 ± 0.2	3S_1	35.6 ± 0.2	(1.17,3.51)	39.7 ± 0.2	99.95(1)	0.051(1)	$8.8(1) \times 10^{-5}$
β -D-Man	13.1 ± 0.4	${}^O S_2$	32.9 ± 0.4	(1.17,2.66)	42.7 ± 0.5	99.58(1)	0.42(1)	$1.41(3) \times 10^{-4}$
β -D-All	12.5 ± 0.2	3O_B	21.8 ± 0.2	(1.22,3.19)	36.8 ± 0.3	99.31(1)	0.68(1)	$9.23(1) \times 10^{-3}$
β -D-Tal	11.9 ± 0.3	B_{30}	43.2 ± 0.1	(1.11,3.40)	46.8 ± 0.2	99.53(1)	0.47(1)	$3.0(1) \times 10^{-6}$
β -D-Gul	13.3 ± 0.3	${}^O S_2$	31.5 ± 0.4	(1.17,3.19)	45.9 ± 0.5	99.00(2)	0.99(1)	$3.4(1) \times 10^{-4}$
β -D-Alt	6.1 ± 0.1	${}^O S_2$	24.7 ± 0.1	(1.17,3.72)	43.8 ± 0.2	93.88(4)	6.12(4)	$2.4(1) \times 10^{-3}$
β -D-Ido	4.1 ± 0.3	B_{25}	27.4 ± 0.2	(1.06,5.85)	44.9 ± 0.2	88.51(9)	11.5(2)	$8.6(1) \times 10^{-4}$
α -D-Glc	16.2 ± 0.2	${}^1S_3-{}^{14}B$	35.1 ± 0.2	(1.22,2.66)	42.5 ± 0.2	99.88(1)	0.124(1)	$8.6(1) \times 10^{-5}$
α -D-Gal	14.5 ± 0.2	1S_3	44.7 ± 0.2	(1.22,3.19)	48.5 ± 0.4	99.58(1)	0.416(5)	$4.0(1) \times 10^{-6}$
α -D-Man	6.5 ± 0.2	${}^O S_2$	22.8 ± 0.1	(1.11,3.19)	32.3 ± 0.3	95.72(3)	4.27(5)	$6.0(1) \times 10^{-3}$
α -D-All	8.1 ± 0.2	$B_{30}-{}^1S_3$	27.1 ± 0.2	(1.17,3.40)	38.9 ± 0.2	97.92(2)	2.08(3)	$8.7(1) \times 10^{-4}$
α -D-Tal	6.8 ± 0.1	${}^O S_2$	33.7 ± 0.2	(1.65,4.47)	52.5 ± 0.2	91.60(6)	8.40(6)	$1.7(1) \times 10^{-4}$
α -D-Gul	4.2 ± 0.2	${}^O S_2$	30.3 ± 0.2	(1.49,3.94)	49.2 ± 0.3	90.44(7)	9.6(1)	$1.2(1) \times 10^{-4}$
α -D-Alt	2.8 ± 0.3	B_{30}	15.0 ± 0.2	(1.06,3.72)	28.9 ± 0.2	79.2(1)	20.7(2)	$8.74(1) \times 10^{-2}$
α -D-Ido	1.1 ± 0.2	${}^O S_2-{}^{14}B$	20.6 ± 0.2	(1.11,5.53)	31.6 ± 0.2	51.8(3)	48.2(2)	$1.38(1) \times 10^{-2}$

Energies are expressed in kJ/mol, and probabilities in percent; ^a Free energy of 1C_4 ; ^b Next most

populated conformer after 4C_1 and 1C_4 ; ^c Free energy of the next most populated conformer; ^d Location of the transition state (θ, ϕ); ^e Free energy of the transition state; ^f Population of 4C_1 (%); ^g Population of 1C_4 (%); ^h Population of the next most populated conformer. When a basin is present, which encompasses many states, all conformers involved are listed.

TABLE V: Free energy and population of different conformers using the new parameter set.